Combinatorial targeting of microRNA-26b and microRNA-101 exerts a synergistic inhibition on cyclooxygenase-2 in brain metastatic triple-negative breast cancer cells

Rania Harati, Aloïse Mabondzo, Abdelaziz Tlili, Ghalia Khoder, Mona Mahfood, Rifat Hamoudi

Breast Cancer Research and Treatment (2021) 187:695–713
https://doi.org/10.1007/s10549-021-06255-y

PRECLINICAL STUDY

Combinatorial targeting of microRNA-26b and microRNA-101 exerts a synergistic inhibition on cyclooxygenase-2 in brain metastatic triple-negative breast cancer cells

Rania Harati[1,2] · Aloïse Mabondzo[3] · Abdelaziz Tlili[4] · Ghalia Khoder[2,5] · Mona Mahfood[4] · Rifat Hamoudi[2,6,7]

Received: 23 November 2020 / Accepted: 4 May 2021 / Published online: 26 May 2021

Abstract

Purpose Extravasation of triple-negative (TN) metastatic breast cancer (BC) cells through the brain endothelium (BE) is a critical step in brain metastasis (BM). During extravasation, metastatic cells induce alteration in the inter-endothelial junctions and transmigrate through the endothelial barrier. Transmigration of metastatic cells is mediated by the upregulation of cyclooxygenase-2 (COX-2) that induces matrix metalloproteinase-1 (MMP-1) capable of degrading inter-endothelial junctional proteins. Despite their important role in BM, the molecular mechanisms upregulating COX-2 and MMP-1 in TNBC cells remain poorly understood. In this study, we unraveled a synergistic effect of a pair of micro-RNAs (miR-26b-5p and miR-101-3p) on COX-2 expression and the brain transmigration ability of BC cells.

Methods Using a gain-and-loss of function approach, we modulated levels of miR-26b-5p and miR-101-3p in two TNBC cell lines (the parental MDA-MB-231 and its brain metastatic variant MDA-MB-231-BrM2), and examined the resultant effect on COX-2/MMP-1 expression and the transmigration of cancer cells through the BE.

Results We observed that the dual inhibition of miR-26b-5p and miR-101-3p in BC cells results in higher increase of COX-2/MMP-1 expression and a higher trans-endothelial migration compared to either micro-RNA alone. The dual restoration of both micro-RNAs exerted a synergistic inhibition on COX-2/MMP-1 by targeting COX-2 and potentiated the suppression of trans-endothelial migration compared to single micro-RNA.

Conclusion These findings provide new insights on a synergism between miR-26-5p and miR-101-3p in regulating COX-2 in metastatic TNBC cells and shed light on miR-26-5p and miR-101-3p as prognostic and therapeutic targets that can be exploited to predict or prevent BM.

Keywords miR-26b · miR-101 · COX-2 · Breast cancer · Brain metastasis · Blood–brain barrier

✉ Rania Harati
rharati@sharjah.ac.ae

Aloïse Mabondzo
aloise.mabondzo@cea.fr

Abdelaziz Tlili
atlili@sharjah.ac.ae

Ghalia Khoder
gkhoder@sharjah.ac.ae

Rifat Hamoudi
rhamoudi@sharjah.ac.ae; r.hamoudi@ucl.ac.uk

[1] Department of Pharmacy Practice and Pharmacotherapeutics, College of Pharmacy, University of Sharjah, 27272, Sharjah, United Arab Emirates

[2] Sharjah Institute for Medical Research, University of Sharjah, 27272, Sharjah, United Arab Emirates

[3] Department of Medicines and Healthcare Technologies, The French Alternative Energies and Atomic Energy Commission, Paris-Saclay University, 91191 Gif-sur-Yvette, France

[4] Department of Applied Biology, College of Sciences, University of Sharjah, 27272, Sharjah, United Arab Emirates

[5] Department of Pharmaceutics and Pharmaceutical Technologies, College of Pharmacy, University of Sharjah, 27272, Sharjah, United Arab Emirates

[6] Clinical Sciences Department, College of Medicine, University of Sharjah, 27272, Sharjah, United Arab Emirates

[7] Division of Surgery and Interventional Science, University College London, London W1W 7EJ, UK

Introduction

Brain metastasis is an incurable end-stage of breast cancer and remains invariably a major cause of morbidity and mortality in spite of the major advances that have been made by systemic therapies [1]. The metastatic potential of BC cells as well as their response to therapy varies with the molecular subtype of the disease; each molecular subtype displays distinct patterns of metastatic spread with notable differences in survival after relapse [2]. Brain metastasis develops more frequently in triple-negative (25%-27%) and HER2 + subtypes (11%-20%), while the incidence of BM in hormone receptor-positive is much lower (8%-15%) [2, 3]. BM in patients with the TN subtype is associated with the worse median survival (3–4 months) due to several factors including the absence of approved effective targeted therapy [4]. Despite its clinical importance, the molecular mechanism of brain metastasis remains poorly understood. Understanding the biology of BM and the molecular makeup of tumor cells, particularly TNBC, more prone to disseminate to the brain, will open avenues for both the prediction of patients at high risk to develop BM and the discovery of new drug targets.

Brain metastasis is a complex process during which cancer cells detach from the primary tumors, survive in the bloodstream, cross the blood–brain barrier (BBB) and finally colonize the brain [5]. One of the critical steps in breast cancer brain metastasis (BCBM) is the passage of BC cells through the BBB, a process known as extravasation. The BBB is a unique multicellular structure located at the level of brain microvasculature at the interface between the blood and the brain. It is composed of brain endothelial cells (BEC), pericytes, astrocytes, and a basement membrane. The brain endothelial cells are considered the key element restricting the barrier permeability [6]. Unlike their homologue in the periphery, the BEC are tightly attached to each other by junctional complexes, comprising tight and adherens junctions that restrict the paracellular permeability and make the BBB one of the tightest barriers in the body. The tight junctions (TJ) completely seal the inter-endothelial cleft, while the adherens junctions (AJ) maintain contact between neighboring endothelial cells. Structurally, the TJ complexes are composed of transmembrane proteins (including occludin, claudins (1-, 3-, and -5) and junctional adhesion molecule (JAM)) connected to the actin cytoskeleton via cytoplasmic plaque proteins (including Zonula Occludens (ZO-1, -2, and -3)). Adherens junctions are located below the tight junctions and are composed of transmembrane proteins (including cadherins) linked to the cytoskeleton by cytoplasmic proteins (including catenins) [6, 7]. During extravasation, BC cells adhere to the brain endothelium, induce changes in the inter-endothelial tight junctional proteins (including occludin, claudin-5, and ZO-1) [8, 9] and adhesion junctional proteins (including the VE-cadherin/catenin complex) [10], and then transmigrate between two neighboring cells to reach the brain. Disruption of TJs and AJs by tumor cells increases the BBB permeability and allows the paracellular passage of cancer cells through the endothelial barrier [5]. However, the molecular mechanism by which BC cells acquire their migrative properties allowing them to induce alteration in the inter-endothelial junctions and cross the BBB remains poorly understood.

The cyclooxygenase-2 (COX-2)/matrix metalloproteinase-1 (MMP-1) pathway was shown to play a critical role in the extravasation of TNBC cells through the BBB. TNBC patients with high COX-2 and MMP-1 were found to have the greatest risk of brain metastasis [11]. Mechanistic studies revealed that brain metastatic cells express high levels of COX-2 and MMP-1 compared to primary tumor cells [12] and that overexpression of COX-2 promotes brain metastasis by inducing MMP-1 expression [11] which in turn degrades the inter-endothelial junctions, enhances the BBB permeability, and allows the transmigration of metastatic cells through the brain endothelium [11, 13]. Despite their important role in brain metastasis, the molecular mechanisms leading to upregulation of COX-2/MMP-1 in TN brain metastatic cells remain poorly understood. A better understanding of these molecular mechanisms will open avenues for better prognostic and therapeutic strategies.

In recent years, micro-RNAs have emerged as important regulators of gene expression. Micro-RNAs are a class of non-coding RNA that negatively regulate gene expression at mRNA and protein level [14]. Dysregulation of micro-RNAs is involved in tumorigenesis, metastasis, and drug resistance [15, 16]. In case of BCBM metastasis, brain metastatic tumors were shown to express distinct micro-RNAs signature compared to primary tumors, suggesting a potential role of micro-RNAs dysregulation in the development of brain metastases. In a previous study, we showed that miR-101-3p is downregulated in TN brain metastatic breast cancer cells which upregulates COX-2 and increases the transmigration of metastatic cells through the brain endothelium. Restoring miR-101-3p in brain metastatic cells reduces tumor cells migration by directly targeting and reducing COX-2 expression, however, without total suppression of cancer cells transmigration (11).

Mechanistic studies on micro-RNAs action revealed that the 3′UTR of genes are frequently targeted by multiple micro-RNAs and that simultaneous modulation of miRNA pairs can exert synergistic effects on the target genes leading to a potentiation of their biological effects compared to single micro-RNAs [17–22]. Interestingly, a pair of micro-RNAs (miR-101-3p and miR-26b-5p), shown to target COX-2 (PTGS2) gene in multiple types

of cancers [23–28], are both downregulated in brain metastatic tumors compared to primary tumors [29]. Based on these data, we hypothesized that a combinatorial targeting of miR-101-3p and miR-26b-5p might exert a synergistic repression on COX-2 gene in TN metastatic cancer cells and suppress their transmigration through the brain endothelium to a greater extent than single micro-RNA. To test this hypothesis, we compared the anti-transmigrative effect of miR-101 and miR-26b alone and in combination in in vitro models of brain endothelial barrier.

Materials and methods

Animals

Adult female mice ([C57BL/6 J], 8–10 weeks of age) were purchased from Jackson Laboratory (USA) and maintained at the accredited animal facility in the University of Sharjah (UOS). All experiments were approved by the UOS animal care and use committee and conducted according to the UOS directives for animal care.

Cell lines

The non-metastatic (ER^+, $PR^{\pm}$, $HER2^-$) MCF-7 and the triple-negative MDA-MB-231 human breast carcinoma cell lines were obtained from American Type Culture Collection (Rockville, MD). The TN brain metastatic MDA-MB-231-BrM2 cell variant and the parental MDA-MB-231-TGL cells with low brain metastatic propensity were obtained from Dr Joan Massagué (Memorial Sloan-Kettering Cancer Center, New York, USA). The MDA-MB-231-BrM2 cells have an increased propensity to form brain metastases and were isolated from the brain of nude mice following multiple injections of the parental MDA-MB-231-TGL into the internal carotid artery [12]. Cells were cultured in Dulbecco's Modified Eagle Medium (DMEM) supplemented with 10% FBS, 1X L-Glutamine, and antibiotics (1000 U Penicillin/1000 U Streptomycin). The human cerebral microvascular endothelial cell line (hCMEC/D3) was obtained from Cedarlane (Tebu-Bio, France) and cultured in EndoGRO™-MV Complete Medium (cat# SCME004, EMD Millipore, USA) supplemented with 1 ng/mL FGF-2 (cat# GF003, EMD Millipore) and antibiotics. hCMEC/D3 were cultured on flasks pre-coated with thin collagen I (cat# 08–115, EMD Millipore) and fibronectin (cat# F1141, Sigma-Aldrich) coating. All cells were cultured in a humidified incubator with 5% CO_2 at 37 °C and regularly tested for mycoplasma contamination and phenotypic changes.

Establishment of in vitro *brain endothelial barriers from hCMEC/D3 cell line*

To establish the endothelial barriers from hCMEC/D3 cells, (5×10^4) cells were seeded on the upper side of a collagen and fibronectin-coated polyester Transwell membrane (Costar, pore size 8 µm; growth area 1.12 cm^2) in endothelial basal medium (EndoGRO™-MV Complete Medium). Under these experimental conditions, brain endothelial cells form a confluent monolayer within 72 h with the highest transendothelial electrical resistance (TEER) values between days 3 and 7 [30, 31].

Establishment of in vitro *brain endothelial barriers from primary cells*

Primary brain endothelial cells were isolated from adult female mice ([C57BL/6 J], 8–10 weeks of age) as previously described [32, 33]. The purity of isolated brain endothelial cells was examined by measuring the gene expression of three cell markers: CD31 or pecam-1 (marker of endothelial cells), glial fibrillary acidic protein or gfap (marker of glial cells), and α-actin or acta2 (marker of pericytes). The following mouse primers from Macrogen (South Korea) were used: Pecam1 Mouse qPCR Primer Pair (NM_008816), F: CCAAAGCCAGTAGCATCATGGTC, R: GGATGG TGAAGTTGGCTACAGG; Gfap Mouse qPCR Primer Pair (NM_010277), F: CACCTACAGGAAATTGCTGGAGG, R: CCACGATGTTCCTCTTGAGGTG; Acta2 Mouse qPCR Primer Pair (NM_007392), F: TGCTGACAGAGG CACCACTGAA, R: CAGTTGTACGTCCAGAGGCATAG. To establish the endothelial barriers from primary cells, (5×10^4) of isolated BEC cells were seeded on the upper side of a collagen and fibronectin-coated polyester transwell membrane (Costar, pore size 8 µm; growth area 1.12 cm^2) in endothelial basal medium (EGM-2MV Endothelial Med BulletKit, cat # CC-3202, Lonza, Switzerland) containing 0.1% human recombinant epidermal growth factor (hEGF), 0.04% hydrocortisone, 0.1% human recombinant insulin-like growth factor, 0.1% ascorbic acid, 0.1% gentamicin, 0.1% amphotericin-BN, and 5% fetal bovine serum). Under these experimental conditions, brain endothelial cells form a confluent monolayer within 12 days.

Transendothelial electric resistance (TEER) measurement

TEER of endothelial barriers was measured with an Endohm 12 chamber and an Endohmeter EVOMX (World Precision Instruments). Media were refreshed and inserts were kept at room temperature for 20 min prior to TEER measurement to exclude interference of temperature and media. Background of the coated transwell membrane and medium

was subtracted from each reading. The TEER values were expressed as Ω.cm^2 (surface area of the Transwell inserts).

Cell transfection

To introduce miR-26b-5p and miR-101-3p, cells were transfected with 2.5 nM of miR-26b-5p mimic (Syn-hsa-miR-26b-5p miScript miRNA Mimic, Cat# 219,600, MSY0000083: 5′UUCAAGUAAUUCAGGAUAGGU, Qiagen, Germany), miR-101-3p mimic (Syn-hsa-miR-101-3p miScript miRNA Mimic, Cat# 219,600, MSY0000099: 5'UACAGUACUGUGAUAACUGAA, Qiagen), or its (scrambled) control (AllStars Negative Control, cat# SI03650318, Qiagen) using HiPerFect transfection agent (Qiagen) in culture media for 48 h. For inhibition studies, 15 nM of miR-26b-5p inhibitor (Anti-hsa-miR-26b-5p miScript miRNA Inhibitor, cat# 219,300, MIN0000083), miR-101-3p inhibitor (Anti-hsa-miR-101-3p miScript miRNA Inhibitor, cat# 219,300, MIN0000099), or its negative control (miScript Inhibitor Negative Control, cat# 1,027,271, Qiagen) were transfected using HiPerFect transfection agent in culture media for 48 h. Down- and upregulation of miR-26b-5p and miR-101-3p were assessed by QPCR.

Cell viability assay

MDA-MB-231 cells (5×10^3 cell/well) were seeded in 96-well plate. After 24 h, cells were treated with 20 µM of celecoxib (ab141988, abcam). Six hours later, cells were transfected with miR-26b-5p and miR-101-3p mimics or inhibitors, and cell viability was measured by MTT (3-(4,5-dimethylthiazol-2-yl)-2,5-diphenyltetrazolium bromide) assay after 48 h; 100 µL of MTT (5 mg/mL) was added and cells were incubated for 4 h. Supernatant was then removed and 50 µL of DMSO (dimethyl sulfoxide) was added to each well. The absorbance was measured at 540 nm wavelength using Multiskan Go microplate spectrophotometer (Thermo Fisher, Waltham, MA, USA).

Quantitative real-time PCR

Total RNAs were extracted from cells using the miRNeasy Micro Kit (cat# 217,084, Qiagen, Germany) following the manufacturer's instructions. micro-RNAs were reversed transcribed into cDNA using the miScript II RT Kit (cat# 218,161) from Qiagen. mRNAs were reversed transcribed using the RT^2 First Strand Kit (Cat#, 330,401, Qiagen). The miScript SYBR Green PCR Kit (Cat# 218,075) was used to detect miRNA expression, and the RT^2 SYBR Green ROX qPCR Mastermix (cat# 330,522) was used for mRNA expression according to the manufacturer's protocol. PCR amplifications were performed on the "Applied Biosystems® StepOne™ Real-Time PCR System." The specific primers from Qiagen were as follows: Hs_miR-26b_1 miScript Primer Assay (Cat# MS00003234), Hs_miR-101_3 miScript Primer Assay (Cat# MS8300072), RT^2 qPCR Primer Assay for Human PTGS2 (cat# PPH01136F), and RT^2 qPCR Primer Assay for Human MMP1 (cat# PPH00120B-200). Hs_RNU6-2_11 miScript Primer Assay (cat# MS00033740) and RT^2 qPCR Primer Assay for Human GAPDH (Cat# PPH72843A) were used as internal control for miRNA and mRNA, respectively. The specificity of each reaction was assessed by melting curve analysis. The relative gene expression was determined using the $2^{-\Delta Ct}$ and $2^{-\Delta\Delta Ct}$ methods [34].

Trans-endothelial migration assay

Trans-endothelial migration assay was performed as previously described [35]. hCMEC/D3 and primary brain endothelial cells were plated on the upper side of an 8 µm pore size insert, pre-coated with collagen and fibronectin. On the day of the experiment, TEER was monitored to assess the monolayer tightness. TEER values of control endothelial monolayers hCMEC/D3 were around 70 Ω cm^2 between days 5 and 7 of culture. Chambers with a TEER lower than 65 Ω cm^2 were discarded. TEER values of control primary brain endothelial cells were around 500 Ω cm^2 on day 12 of culture. For transmigration assay, 5×10^4 transfected or control cells were pre-labeled with 5 µM of CellTracker™ Green CMFDA fluorescent dye (cat# C2925, Thermo Fisher Scientific, USA) and then added gently to the apical (upper) side of the transwell. Four hours later, non-adherent cells were washed with PBS. After 24 h, TEER was measured again and non-migrated cells remaining in the upper chamber were carefully removed with a cotton swab. Cancer cells that have transmigrated through the brain endothelium to the basal compartment were fixed with 4% PFA for 20 min for imaging and counting under Olympus BX43 fluorescence microscope, or lysed with RIPA 1X buffer for fluorescence quantification [28, 36]. The fluorescence signal in the lower compartment was quantified in Varioskan Flash microplate reader (Thermo Fisher scientific) at wavelength excitation/emission: 492/517 nm.

Cell sorting and western blot

Protein expression of COX-2 and MMP-1 in cancer cells as well as the inter-endothelial junctions (Claudin-5, VE-cadherin, ZO-1, and β-catenin) in brain endothelial cells was assessed by western blot following standard procedures and as previously described [28]. To measure the expression of inter-endothelial junctions in BECs, MDA-MB-231-TGL and MDA-MB-231-Brm2 cells, which are stably transduced with a lentivirus expressing a triple fusion reporter (TGL) encoding herpes simplex virus thymidine kinase

1, green fluorescent protein (GFP) and firefly luciferase [12], were co-cultured with hCMEC/D3 cells. After 24 h of co-culture, cells were collected with accutase (Corning, USA) and sorted with the BD FACSAria™ III cell sorter (BD Biosciences, USA) using the 488 nm laser to separate GFP-expressing cancer cells from unlabeled hCMEC/D3. The following primary antibodies from Abcam were used: Anti-COX-2 (ab15191) 1/1000, Anti-MMP-1 (ab38929) 1/5000, Anti-Claudin-5 (ab15106) 1/500, Anti-VE Cadherin (ab33168) 1/1000, Anti-ZO-1 (ab216880) 1/1000, and Anti-β-catenin (ab32572) 1/3500. Anti-GAPDH (ab9485) 1/7500 was used as loading and transfer control.

Immunofluorescence

Cells were fixed with 4% paraformaldehyde for 10 min and permeabilized with 0.15% Triton™ X-100. After blocking with 2% BSA for 1 h, cells were incubated overnight at 4 °C with anti-COX-2 primary antibody (ab15191) 1/500. Cells were then washed and incubated for 1 h with secondary antibody donkey F(ab′)2 anti-rabbit IgG H&L (Phycoerythrin) (ab7007) 1/200. Samples were then mounted in ProLong® Gold Antifade Reagent with DAPI (cat# 8961, Cell Signaling, USA) and examined with Olympus BX43 fluorescence microscope.

Enzyme-linked immunosorbant assay (ELISA)

Culture supernatants of transfected BC cells were collected and frozen at − 20 °C. For quantification of Prostaglandin E_2 (PGE2) and MMP-1 levels, the Prostaglandin E_2 Parameter Assay Kit (cat# KGE004B, R&D Systems) and the Human Total MMP-1 DuoSet (cat# DY901B, R&D Systems) were used, respectively, according to manufacturer's instructions. The detection limits for PGE2 were 39 pg/mL and for MMP1 were 62.5 pg/mL. Signal saturation was observed at concentrations > 2500 pg/mL for PGE2 and > 4000 pg/mL for MMP-1. The optical density was measured using a Multiskan™ GO Microplate Spectrophotometer (Thermo Scientific, USA) at a wavelength of 450 nm. PGE2 and MMP-1 concentrations were then calculated by generating a four parameter logistic (4-PL) curve-fit.

Dual luciferase reporter assay

For miR-26b target validation, the wild-type (WT) putative binding site of miR-26b-5p in the 3′UTR of COX-2 predicted by TargetScan (version 7.2) (position 257–264 of COX-2 3′ UTR), and the mutant (Mut) 3′UTR of COX-2 with the seed region deleted were cloned into pmirGLO Dual-Luciferase miRNA Target Expression Vector (pmirGLO-empty, Promega, USA) downstream of the firefly luciferase gene (XbaI sites) to obtain Luc Reporter Constructs. The following primers were used for cloning: 26_PTGS2_WT_F: 5′CTAGACCAGAGAGAAATGAGTTTTGAC GTCTTTTTACTTGAATTTCAACTTATATTATAAGAACGAAAGTAA3′; 26_PTGS2_WT_R 5′CTAGTT ACTTTCGTTCTTATAATATAAGTTGAAATTCAAGTAAAAAGACGTCAAAACTCATTTCTCTCTGGT3′(WT). The mutant primers were: 26_PTGS2_MUT_F: 5′CTAGACCAGAGAGAAATGAGTTTTGACGTCTTT TTTTCAACTTATATTATAAGAACGAAAGTAA3′; 26_PTGS2_MUT_R 5′CTAGTT ACTTTCGTTCTTATAA TATAAGTTGAAAAAAAGACGTCAAAACTCATTTCTCTCTGGT3′ (MUT). For miR-101-3p target validation, the wild-type (WT) putative binding site of miR-101-3p in the 3′UTR of COX-2 predicted by TargetScan 7.2 (position 1738–1744 of PTGS2 3′ UTR) and the mutant (MUT) 3′UTR of COX-2 with the seed region deleted were cloned into pmirGLO Dual-Luciferase miRNA Target Expression Vector as previously described [28]. The following primers were used:

101_PTGS2_WT_F 5′CTAGCCACATCTCATTGTCACTGACATTTAATGGTACTGTATATTACTTAATTTATTGAAGATTATTATTTA3′; 101_PTGS2_WT_R 5′CTAGTAAATAATAATCTTCAATAAATTAAGTAATATACAGTACCATTAAATGTCAGTGACAATGAGATGTGG3′;

101_PTGS2_MUT_F 5′CTAGCCACATCTCATTGTCACTGACATTTAATGGATTACTTAATTTATTGAAGATTATTATTTA3′; 101_PTGS2_MUT_R 5′CTAGTAAATAATAATCTTCAATAAATTAAGTAATCCATTAAATGTCAGTGACAATGAGATGTGG3′.

MDA-MB-231 cells (ATCC) were plated at a density of 10^4 cells/well in a 96-well plate and co-transfected with pmirGLO-Mut (50 ng), pmirGLO-WT (50 ng), miR-26 mimic (10 nM), and/or miR-101 mimic (10 nM) or negative scrambled control depending on treatments, and following Lipofectamine 3000 reagent protocol. 24 h after transfection, cell lysates were harvested and used to sequentially measure the Firefly and Renilla luciferase activities using the Dual-Luciferase® Reporter Assay System analysis (cat# E2940, Promega, USA) according to the manufacturer's instructions. Firefly activities were normalized with Renilla luciferase.

Statistical analysis

Data are expressed as mean ± SD (standard deviation) from three or four independent experiments with (2–3) replicates each. Unpaired Student's *t* test was used for statistical comparison between two groups, and one-way ANOVA followed by Bonferroni post hoc test was used for comparison among multiple groups. Differences were considered to be statistically significant at probability levels of $p < 0.05$(*), $p < 0.01$(**), and $p < 0.001$(***). Calculations and figures were generated using the statistical software GraphPad Prism (version 8.2.0).

To identify whether the combination had a synergistic effect, the Combination Index (CI) was calculated according to the Chou-Talalay method [37–40]. Cells were treated with a combination of miR-26b and miR-101 mimics using the method of constant ratio drug combination proposed by Chou and Talalay. The two mimics were used at the concentration of 1.25, 2.5, and 5 nM each. Then using gene expression data from real-time PCR, the CI values for each mimic pair were calculated using the CompuSyn algorithm. CI < 1 denotes a synergism; CI = 1 denotes an addition, and CI > 1 denotes an antagonism.

Results

Breast cancer cells with high brain metastatic propensity express lower levels of miR-26b-5p and miR-101-3p compared to non-metastatic cells

Previous studies showed that two micro-RNAs (miR-26b-5p and miR-101-3p), known to target the 3′UTR of COX-2, are significantly downregulated in brain metastatic tumors compared to primary tumors in patients samples [29]. We measured the expression levels of miR-26b-5p and miR-101-3p by real-time PCR in three breast cancer cell lines with different brain metastatic propensities: MCF-7 (ER^+, $PR^\pm$, $HER2^-$, non-metastatic), MDA-MB-231-TGL (MDA-231 for brevity, TN, metastatic), and MDA-MB-231-BrM2 (MDA-231-BrM for brevity, TN, brain metastatic). Our results showed that levels of both micro-RNAs, miR-26b-5p and miR-101-3p, were lower in TN MDA-231-BrM cells compared to parental TN MDA-231 (miR-26: fold change = 0.28, $p = 0.0475$; miR-101: fold change = 0.01) and non-metastatic (ER^+, $PR^\pm$, $HER2^-$) MCF-7 (miR-26: fold change = 0.13, $p = 0.0004$; miR-101: fold change = 0.002, $p = 0.0011$) (Fig. 1). These results are in accordance with previous results obtained from patients' samples showing that miR-101-3p and miR-26b-5p are significantly downregulated in brain metastatic tumors compared to primary tumors [29], which suggests that loss of these micro-RNAs could exert a potential role in brain metastasis.

MiR-26b-5p and miR-101-3p cooperatively target the 3′-UTR of COX-2 mRNA in breast cancer cells

The 3′UTR of COX-2 (PTGS2) mRNA was shown to be targeted by miR-26b-5p or miR-101-3p in multiple types of cancer [23–28]. The putative target sequences of miR-26b-5p and miR-101-3p in the 3′UTR of COX-2 mRNA predicted by TargetScan 7.2 are shown in Fig. 2a and b. We conducted luciferase reporter assays in MDA-MB-231 cells to confirm the previous observations. miR-26b-5p or miR-101-3p mimics were co-transfected with luciferase constructs containing the putative (wild-type WT) or mutated (Mut) binding site of miR-26b-5p (pmirGlo-PTGS2 (seed-miR-26)-3′UTR) and miR-101-3p (pmirGlo-PTGS2 (seed-miR-101)-3′UTR) in the 3′UTR of COX-2. For the luciferase assay, we used MDA-MB-231 cells (from ATCC) with no endogenous luciferase activity; the two other cell lines, MDA-MB-231-TGL and MDA-MB-231-BrM2, could not be used as they are stably transduced with a lentivirus expressing a triple fusion reporter (TGL) encoding firefly luciferase. The luciferase assays showed that mimics of both micro-RNAs significantly reduced the luciferase activity in cells transfected with the pmirGlo-PTGS2-3′UTR-WT construct compared to control cells (miR-26b-5p: 43.14% reduction, $p < 0.0001$; miR-101-3p: 34.07% reduction, $p < 0.0027$), whereas the two mimics had no inhibitory effects on luciferase activity in cells transfected with construct containing mutated seed sequences (Fig. 2a and b). These data confirmed results obtained from previous studies showing that miR-26b-5p and miR-101-3p directly target COX-2 mRNA which suggests a potential role of these micro-RNAs in regulating COX-2 expression in metastatic breast cancer cells.

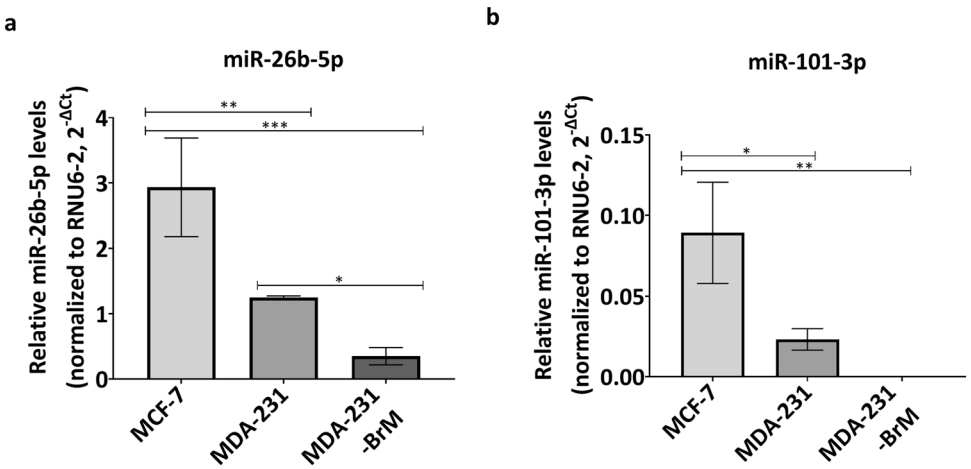

Fig. 1 miR-26b-5p and miR-101-3p levels are reduced in brain metastatic breast cancer cells compared to non-metastatic cells. Expression levels of miR-26b-5p (**a**) and miR-101-3p (**b**) in breast cancer cells with different brain metastatic propensities measured by real-time PCR. The small nuclear RNA (RNU6-2) was used as an internal standard. Data represent mean ± SD from three independent experiments. *$p < 0.05$, **$p < 0.01$, ***$p < 0.001$

Interestingly, the combination of miR-26-5p and miR-101-3p mimics results in greater reduction of the luciferase activity in cells co-transfected with both constructs containing the putative seed sequences of miR-26b-5p and miR-101-3p and this by around 77.64% ($p < 0.0001$) compared to control treatment (Fig. 2c). In comparison to single transfections, the combination (miR-26-5p and miR-101-3p) reduced the luciferase signal by around 35.25% ($p < 0.0001$) compared to miR-26b-5p and by around 45.30% ($p < 0.0001$) compared to miR-101-3p (Fig. 2c). These results suggested that the combination (miR-26-5p and miR-101-3p) tend to synergistically regulate the COX-2 expression in BC cells.

The dual loss of miR-26 and miR-101 in TN breast cancer cells produces a higher increase of COX-2/MMP-1 expression compared to either micro-RNA alone

We next investigated the effect of a dual inhibition of miR-26b-5p and miR-101-3p on COX-2 expression in TNBC cells. MDA-MB-231-TGL (MDA-231) cells were transfected with miR-26b-5p inhibitor (15 nM), miR-101-3p inhibitor (15 nM), or both inhibitors (15 nM each) simultaneously. Results are represented in Fig. 3 and show that treatment with miR-26b-5p inhibitor alone significantly reduced miR-26b-5p expression ($p < 0.001$) without affecting miR-101-3p expression, while the co-transfection with both inhibitors significantly reduced expression of miR-26b-5p and miR-101-3p (Fig. 3a). Same observations were made with miR-101-3p inhibitor alone or combined with miR-26b-5p inhibitor ($p < 0.001$) (Fig. 3b). The dual Inhibition of miR-26b-5p or miR-101-3p in MDA-231 cells expressing low levels of COX-2 produced a significant increase of COX-2 gene expression (fold change = 4.10, $p = 0.0003$) that is higher than each micro-RNA alone (Fig. 3c). This higher increase was also observed at the level of protein expression, measured by western blot and immunofluorescent staining where the dual inhibition of both micro-RNAs increased COX-2 expression [fold change = 5.14-fold ($p = 0.0027$) and 5.60 ($p = 0.0041$)] compared to miR-26b-5p or miR-101-3p alone, respectively (Fig. 3d and e). As COX-2 is known to mediate cancer cells transmigration by inducing MMP-1 expression, we assessed expression of MMP-1. Our results showed that the dual inhibition of both micro-RNAs increased MMP-1 protein expression by 3.25-fold and 3.30-fold compared to miR-26b-5p or miR-101-3p alone, respectively (Fig. 3f). Rescue experiments were performed by treating MDA-231 cells with celecoxib (20 µM), a selective COX-2 inhibitor. Six hours later, cancer cells were transfected with miR-26b-5p inhibitor alone, miR-101-3p inhibitor alone, or with both inhibitors simultaneously, and expression of COX-2 and MMP-1 was assessed 48 h later. Results showed that treatment with celecoxib rescued the effect of micro-RNAs inhibition on COX-2 and MMP-1 expression (Supplementary Figures S1). In addition, we assessed the effect of micro-RNAs inhibition and celecoxib treatment on cell viability as previous studies reported that celecoxib reduces viability of BC cells at high doses (40 µM) [41]. Our results represented in (Supplementary Figures S2) showed that treatment of cancer cells with celecoxib at the dose of 20 µM and miR-26b-5p and miR-101-3p inhibitors (15 nM) does not significantly affect cell viability. Taken together, these results showed that miR-26 and miR-101 cooperatively target COX-2 in breast cancer cells, and the dual inhibition of both micro-RNAs produces a higher increase of COX-2/MMP-1 expression compared to either micro-RNA alone.

The dual inhibition of miR-26 and miR-101 in TN breast cancer cells results in greater increase of the transmigration of BC cells through the brain endothelium compared to either micro-RNA alone.

We next evaluated the effect of miR-26b-5p and miR-101-3p dual inhibition on the transmigration of MDA-231 cells through the brain endothelium. Two models of in vitro brain endothelial barriers were established using primary brain endothelial cells or the immortalized human hCMEC/D3 cell line known to retain the morphological characteristics of primary BEC and to form a tight monolayer [30, 31]. Results are represented in Fig. 4 and show that mono-transfection of BC cells with 15 nM of miR-62b-5p or miR-101-3p inhibitors alone do not cause a significant increase in the transmigration of BC cells through the primary brain endothelium compared to negative control, while the dual inhibition of both micro-RNAs resulted in significantly higher increase of trans-endothelial migration by 2.71-fold ($p = 0.003$) compared to negative control and by 2.12-fold ($p = 0.0074$) and 2.06-fold ($p = 0.0129$) compared to miR-26b-p and miR-101-3p, respectively (Fig. 4a). Using the *in vitro* model of brain endothelial barriers established with hCMEC/D3 cells, results showed that trans-endothelial migration of BC cells was increased by 2.51-fold ($p = 0.0049$) and 2.93-fold ($p = 0.0092$) when MDA-231 cells were mono-transfected with miR-26b-5p or miR-101-3p alone, respectively, while co-transfection with both micro-RNAs further increased transmigration of cancer cells by 6.95 times ($p < 0.001$) compared to control and by 2.77 times ($p = 0.0006$) and 2.38 times ($p = 0.0019$) compared to either miR-26b-p or miR-101-3p, respectively (Fig. 4b and c). Rescue experiments showed that treatment with celecoxib rescued the effect of micro-RNAs inhibition on the trans-endothelial migration (Supplementary Figures S3). Taken together, these results show that the dual inhibition of miR-26b-5p and miR-101-3p produces a higher increase in COX-2 expression which results in greater transmigration of BC cells through the

a

Position 257-264 of PTGS2 3' UTR	Predicted target sequence of miR-26b-5p in the 3'UTR of PTGS2 mRNA
	5' ..GUUUUGACGUCUUUUUACUUGAA...
hsa-miR-26b-5p	3' UGGAUAGGACUUAAUGAACUU

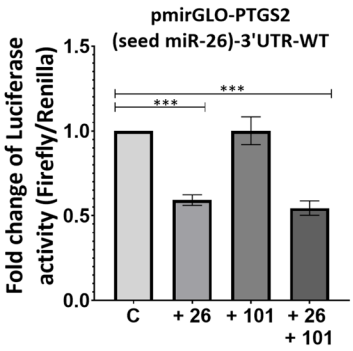

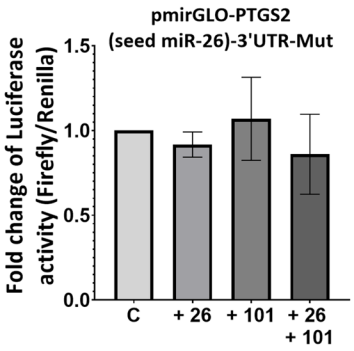

C = Control (Scrambled)

+26= miR-26b-5p mimic

+101= miR-101-3p mimic

+26 +101= miR-26b-5p mimic + miR-101-3p mimic

b

Position 1738-1744 of PTGS2 3' UTR	Predicted target sequence of miR-101-3p in the 3'UTR of PTGS2 mRNA
	5'...CACUGACAUUUAAUG--GUACUGUA...
hsa-miR-101-3p	3' AAGUCAAUAGUGUCAUGACAU

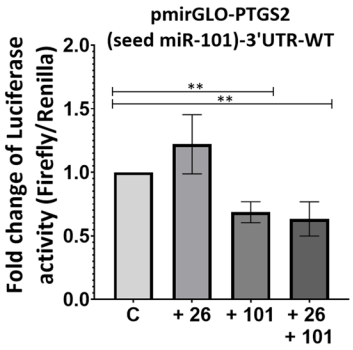

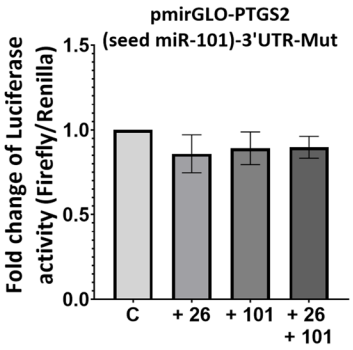

c

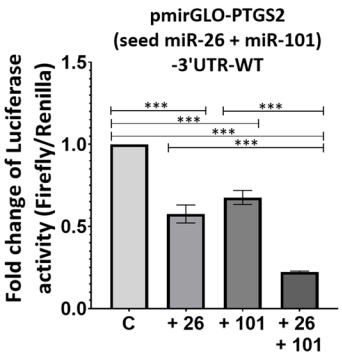

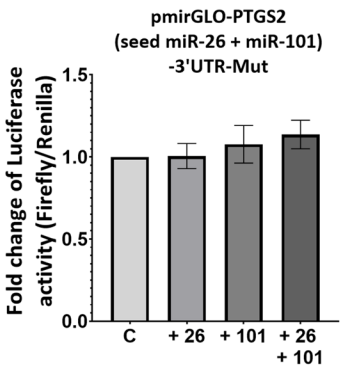

◂**Fig. 2** miR-26b-5p and miR-101-3p cooperatively target the 3'-UTR of COX-2 mRNA. **a** Binding site of miR-26b-5p with the 3′UTR of COX-2 (PTGS2) as predicted by TargetScan (version 7.2). Complementary sequence is represented in blue. Luciferase reporter assay in MDA-MB-231 cells co-transfected with miR-26b-5p mimic (or control) and constructs carrying PTGS2 3′UTR luciferase reporter [pmirGLO-PTGS2 (Seed miR-26b)-3′UTR-WT] or mutant of miR-26b-5p binding site [pmirGLO-PTGS2 (seed miR-26b)-3′UTR-Mut]. **b** Binding site of miR-101-3p with the 3′UTR of COX-2 (PTGS2) as predicted by TargetScan 7.2. Complementary sequence is represented in blue. Luciferase reporter assay in MDA-MB-231 cells co-transfected with miR-101-3p mimic (or control) and constructs carrying PTGS2 3′UTR luciferase reporter [pmirGLO-PTGS2 (Seed miR-101)-3′UTR-WT] or mutant of miR-101-3p binding site [pmirGLO-PTGS2 (seed miR-101)-3′UTR-Mut]. **c** Luciferase reporter assay in MDA-MB-231 cells co-transfected with miR-26b-5p and miR-101-3p mimics (or negative control) and constructs carrying PTGS2 3'UTR luciferase reporter [pmirGLO-PTGS2 (Seed miR-26)-3′UTR-WT and pmirGLO-PTGS2 (Seed miR-101)-3'UTR-WT] or deletion mutant of miR-26b-5p and miR-101-3p binding sites [pmirGLO-PTGS2 (seed miR-26b)-3′UTR-MUT and pmirGLO-PTGS2 (seed miR-101)-3′UTR-Mut]. Data represent mean ± SD from at least three independent experiments. *$p < 0.05$, **$p < 0.01$, ***$p < 0.001$

brain endothelium compared to either micro-RNA alone. We next investigated the effect of miR-26b-5p and miR-101-3p inhibition on the integrity of brain endothelium. Our results showed that co-transfection of MDA-231 cells with both micro-RNA inhibitors results in greater reduction of the TEER compared to each micro-RNA alone (Fig. 5a and b). In primary BECs, co-culture with MDA-231 cells reduced TEER by around 25.42% ($p = 0.0014$) compared to monoculture, while co-culture with MDA-231 cells transfected with either miR-26-5p or miR-101-3p inhibitor alone reduced the TEER by 51.96% ($p = 0.0009$) and 49.48% ($p = 0.002$) compared to control, respectively. Co-culture with MDA-231 cells transfected with both inhibitors further reduced the TEER by 82.58% ($p < 0.001$) compared to control and by 30.62% ($p = 0.0086$) and 33.10% ($p = 0.0106$) compared to cells mono-transfected with either miR-26-5p or miR-101-3p inhibitors, respectively (Fig. 5a). Similar trend was observed using the in vitro model of BECs established with hCMEC/D3 cell line (Fig. 5b). To confirm the effect of both micro-RNAs on the barrier integrity, we evaluated the protein expression of four junctional proteins (claudin-5, VE-cadherin, β-catenin, and ZO-1). Our results showed that these proteins were further reduced when BC cells were transfected with both micro-RNA compared to single inhibition (Fig. 5c-f). Taken together, our data showed that the dual inhibition of miR-26b-5p and miR-101-3p results in greater induction of COX-2/MMP-1 and enhances the transmigration of BC cells through the brain endothelium by exacerbating the disruption of inter-endothelial junctions and further reducing the barrier integrity compared to each micro-RNA alone.

Combination of miR-26b-5p and miR-101-3p exerts a synergistic repressive effect on COX-2 expression in TN brain metastatic BC cells

To determine whether the combination of miR-26b-5p and miR-101-3p exerts a synergistic effect in terms of repressing COX-2 expression, MDA-231-BrM2 cells were first transfected with 1.25 nM, 2.5 nM, or 5 nM of mir-26b-5p mimic alone, mir-101-3p mimic alone, or a combination of mir-26b-5p mimic and mir-101-3p mimic at the same concentrations. Forty-eight hours later, mRNA levels of COX-2 were examined by real-time PCR, and the Combination Index (CI) was calculated according to the Chou-Talalay method [37–40]. Results showed that the different combinations of micro-RNAs at lower concentrations exert a greater repression on COX-2 expression compared to single micro-RNA at higher concentrations, with the greater reduction observed at the combination of 2.5 nM (Supplementary figures S4). Regarding the combination index, our results showed that the CI using 1.25 or 2.5 nM of each mimic are 0.59 and 0.81, respectively, indicating a synergism. However, CI using 5 nM of each mimic is 1.63 indicating an antagonism, which is probably due to an undesirable off-target effect caused by the usage of higher doses of mimics. Indeed, several previous studies showed that transfection of miRNA mimics at high concentrations causes non-specific alterations in gene expression [41, 42]. Based on these first results, the dose 2.5 nM that showed the highest reduction in COX-2 expression was used for the rest of the study to confirm the synergistic effect of miR-26b and miR-101 on COX-2 expression. Indeed, using the concentration of 2.5 nM, transfection with miR-26b-5p mimic alone significantly increased miR-26b-5p expression ($p = 0.0003$) without affecting miR-101-3p expression, while the co-transfection with both mimics significantly increased expression of both miR-26b-5p and miR-101-3p ($p < 0.001$) (Fig. 6a). Same observations were made with miR-101-3p mimic alone or combined with miR-26b-5p mimic (Fig. 6b). Compared to control cells, COX-2 (PTGS2) gene expression was reduced by 3.63-fold in cells transfected with miR-26b-5p alone (fold change = 0.27, $p < 0.001$), by 3.44 times in cells transfected with miR-101-3p mimic (fold change = 0.29, $p < 0.001$), and by 27-fold in cells transfected with both miR-26b-5p and miR-101-3p mimics (fold change = 0.035, $p < 0.001$). The dual inhibition of both micro-RNAs reduced COX-2 gene expression by 7.68-fold (fold change = 0.13, $p = 0.0005$) compared to single mimics (Fig. 6c). Similarly, COX-2 protein levels were more reduced in cells transfected with both mimics (fold change = 0.03, $p = 0.051$) than in cells transfected with either miR-26b-5p (fold change = 0.25, $p = 0.0128$) or miR-101-3p (fold change = 0.25, $p = 0.136$) alone compared to control (Fig. 6d and e). We also measured levels of PGE2 released in culture media. Levels of

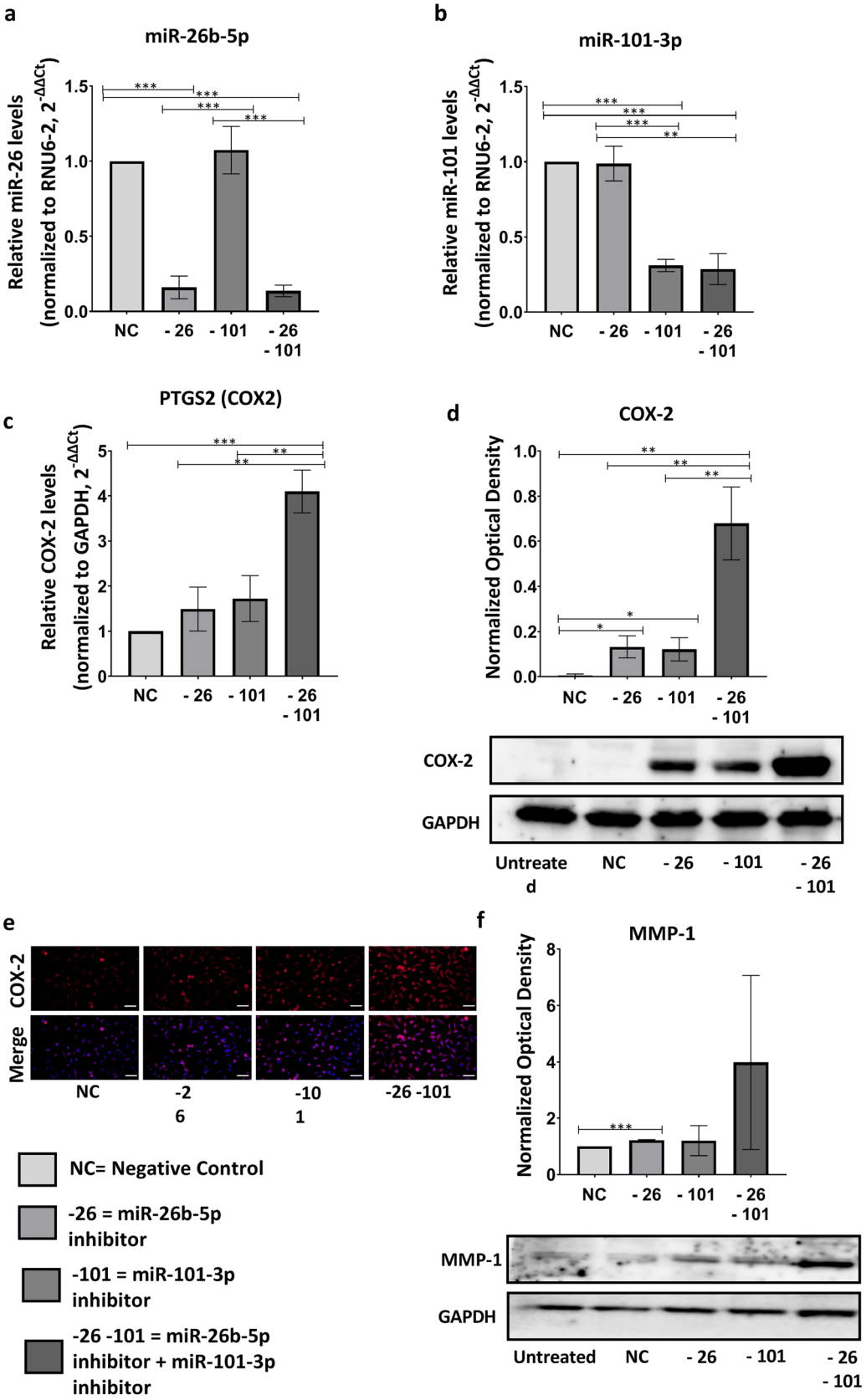
a
miR-26b-5p
Relative miR-26 levels (normalized to RNU6-2, 2^-ΔΔCt)
NC
- 26
- 101
- 26 - 101
b
miR-101-3p
Relative miR-101 levels (normalized to RNU6-2, 2^-ΔΔCt)
c
PTGS2 (COX2)
Relative COX-2 levels (normalized to GAPDH, 2^-ΔΔCt)
d
COX-2
Normalized Optical Density
COX-2
GAPDH
Untreated
e
COX-2
Merge
NC
-26
-101
-26 -101
NC= Negative Control
-26 = miR-26b-5p inhibitor
-101 = miR-101-3p inhibitor
-26 -101 = miR-26b-5p inhibitor + miR-101-3p inhibitor
f
MMP-1
Normalized Optical Density
MMP-1
GAPDH
Untreated

◂**Fig. 3** The dual inhibition of miR-26b-5p and miR-101-3p produces higher increase in COX-2/MMP-1 expression compared to single micro-RNA. MDA-MB-231-TGL cells were transfected with miR-26b-5p/miR-101-3p inhibitors or negative control. **a**,**b** Relative levels of miR-26b-5p (**a**) and miR-101-3p (**b**) measured by real-time PCR. The small nuclear RNA (RNU6-2) was used as an internal standard. **c** Relative levels of COX-2 (PTGS2) mRNA levels measured by real-time PCR. GAPDH was used as an internal standard. **d** Western blot analysis of COX-2 protein. Optical densities were analyzed with Image Lab 6.0.1 software (Bio-Rad) and normalized to GAPDH. **e** Immunofluorescence staining of COX-2. **f** Western blot analysis of MMP-1 protein. Data represent mean ± SD from three independent experiments. Scale bar = 50 µm. *$p < 0.05$, **$p < 0.01$, ***$p < 0.001$

PGE2 were further reduced in cells transfected with both mimics (fold change = 0.03, $p < 0.001$) compared to cells transfected with either miR-26b-5p (fold change = 0.25, $p = 0.0004$) or miR-101-3p (fold change = 0.29, $p = 0.014$) alone compared to control (Fig. 6f). The combination also exerted an enhanced repressive effect on MMP-1 levels. Relative to control cells, MMP-1 protein level was further reduced in cells co-transfected with both inhibitors (fold change = 0.25, $p = 0.066$) compared to cells transfected with miR-26b-5p (fold change = 0.76, $p = 0.0013$) or miR-101-3p (fold change = 0.52) alone (Fig. 6g). Similarly, relative to control cells, levels of MMP-1 released in the media were further reduced in cells co-transfected with both mimics (fold change = 0.05, $p < 0.001$) than with single miR-26b-5p (fold change = 0.56, $p = 0.0092$) or miR-101-3p (fold change = 0.50, $p = 0.0348$) (Fig. 6h). Taken together, these results demonstrate that COX-2/MMP-1 repression was greater when cells are transfected with both micro-RNAs (miR-26b-5p and miR-101-3p) than single micro-RNA.

The combinatorial restoration of miR-26 and miR-101 inhibits the transmigration of TNBC cells through the brain endothelium and preserves the endothelial barrier integrity

We next investigated whether the synergistic effect of combining miR-26b-5p and miR-101-3p on COX-2 repression resulted in greater suppression of BC cells transmigration through the brain endothelium. Relative to control cells, transmigration of cancer cells through primary brain endothelial cells was 37.24% lower when MDA-MB-BrM2 cells are transfected with miR-26b-5p alone ($p < 0.001$), 33.55% lower when MDA-MB-BrM2 cells are transfected with miR-101-3p alone ($p = 0.02$), and 76.75% lower when cells are transfected with the combination of miR-26b-5p and miR-101-3p mimics ($p < 0.001$) (Fig. 7a). Similarly, transmigration of cancer cells through hCMEC/D3 cells was 62.27% lower when MDA-MB-BrM2 cells are transfected with miR-26b-5p alone ($p < 0.001$), 36.99% lower when MDA-MB-BrM2 cells are transfected with miR-101-3p alone ($p = 0.0113$), and 91.70% lower when cells are transfected with the combination of miR-26b-5p and miR-101-3p mimics ($p < 0.001$) (Fig. 7b and c). These results indicate that combining miR-26b-5p and miR-101-3p result in greater suppression of the transmigration of metastatic BC cells through the brain endothelium than did either miR-26b-5p or miR-101-3p alone. We then evaluated effect

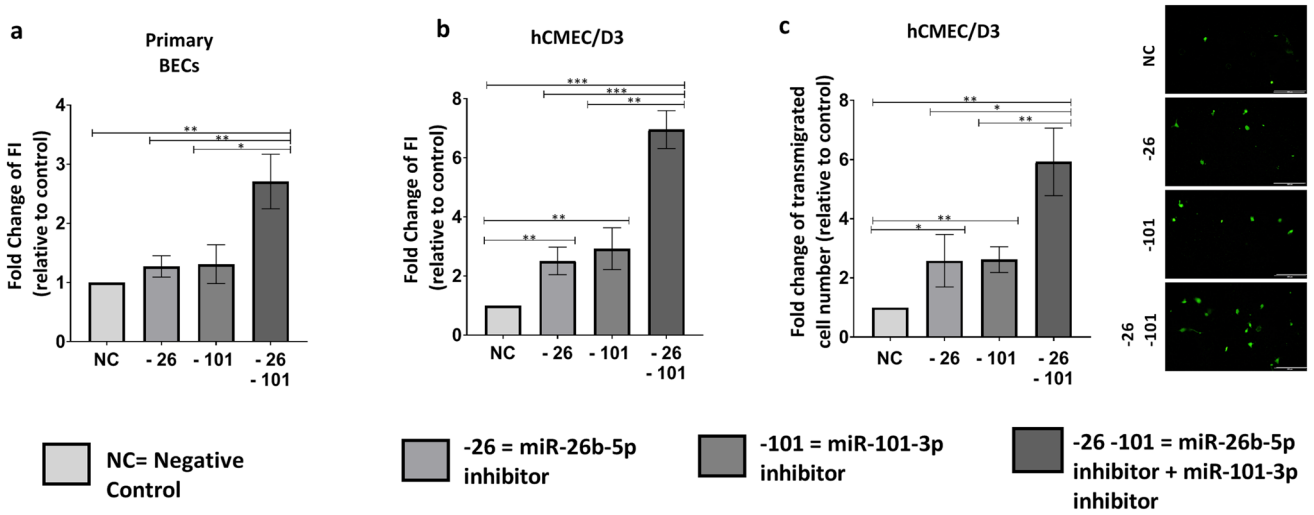

Fig. 4 The dual inhibition of miR-26b-5p and miR-101-3p results in higher transmigration of TNBC cells through the brain endothelium compared to single micro-RNA. **a**,**b** Fluorescently labeled MDA-MB-231-TGL cells transfected with miR-26b-5p/miR-101-3p inhibitors (or negative control) were seeded on top of transwell inserts coated with (**a**) primary BECs or (**b**) hCMEC/D3 cells. The fluorescent intensity in the lower chambers was measured after 24 h. **c** The number of invaded cells was counted in three different fields per insert. Representative images of transmigrated cells (small green cells) are shown. Data represent mean ± SD from three independent experiments. *$p < 0.05$, **$p < 0.01$, ***$p < 0.001$

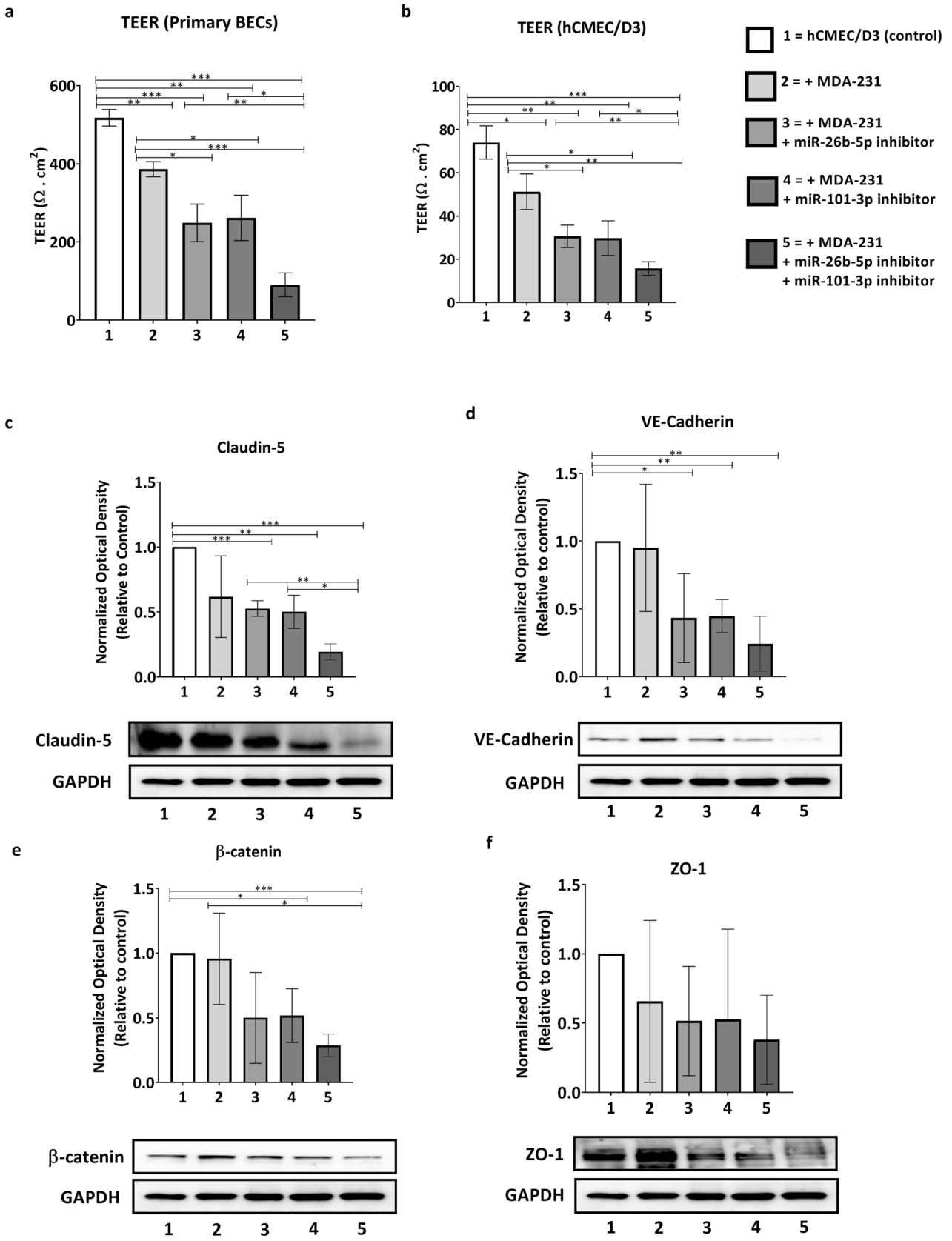
a
TEER (Primary BECs)
TEER (Ω . cm²)
600
400
200
0
1 2 3 4 5
b
TEER (hCMEC/D3)
TEER (Ω . cm²)
100
80
60
40
20
0
1 2 3 4 5
1 = hCMEC/D3 (control)
2 = + MDA-231
3 = + MDA-231 + miR-26b-5p inhibitor
4 = + MDA-231 + miR-101-3p inhibitor
5 = + MDA-231 + miR-26b-5p inhibitor + miR-101-3p inhibitor
c
Claudin-5
Normalized Optical Density (Relative to Control)
1.5
1.0
0.5
0.0
1 2 3 4 5
Claudin-5
GAPDH
1 2 3 4 5
d
VE-Cadherin
Normalized Optical Density (Relative to control)
1.5
1.0
0.5
0.0
1 2 3 4 5
VE-Cadherin
GAPDH
1 2 3 4 5
e
β-catenin
Normalized Optical Density (Relative to control)
1.5
1.0
0.5
0.0
1 2 3 4 5
β-catenin
GAPDH
1 2 3 4 5
f
ZO-1
Normalized Optical Density (Relative to control)
1.5
1.0
0.5
0.0
1 2 3 4 5
ZO-1
GAPDH
1 2 3 4 5

◂**Fig. 5** The dual inhibition of miR-26b-5p and miR-101-3p in TNBC cells exacerbates disruption of the brain endothelium integrity. **a**,**b** Transendothelial electrical resistance (TEER) of primary brain endothelial cells (**a**) or hCMEC/D3 (**b**) co-cultured with MDA-MB-231-TGL cells pre-transfected with miR-26b-5p/miR-101-3p inhibitors or negative control after 24 h of co-culture. **c**–**f** Western blot analysis of the inter-endothelial junctional proteins (claudin-5, VE-cadherin, *β*-catenin, and ZO-1) of hCMEC/D3 cells co-cultured with transfected MDA-MB-231-TGL cells. Optical densities were analyzed with Image Lab 6.0.1 software (Bio-Rad) and normalized to GAPDH. Data are mean ± SD from three independent experiments. $^{*}p < 0.05$, $^{**}p < 0.01$, $^{***}p < 0.001$

of combining miR-26b-5p and miR-101-3p on the barrier integrity and its inter-endothelial junctions. A shown in Fig. 8, combination of both micro-RNAs restores normal TEER values and normal protein levels of inter-endothelial junctions. These results show that the dual restoration of miR-26b-5p and miR-101-3p potentiated the suppression of COX-2 and trans-endothelial migration of metastatic cells, which is in accordance with previous studies showing that the biological effect of micro-RNAs can be potentiated by the synergistic effect of combining two micro-RNAs that target a same gene.

Discussion

In the present study, we provide first-time evidence of a synergistic effect exerted by a pair of micro-RNAs (miR-26b-5p and miR-101-3p) on COX-2 expression in brain metastatic triple-negative breast cancer cells. The dual inhibition of miR-26b-5p and miR-101-3p results in higher increase in COX-2/MMP-1 and grants metastatic cells a higher trans-migrative capacity through the brain endothelium. The combinatorial restoration of both miR-26b-5p and miR-101-3p exerted a synergistic repressive effect on COX-2/MMP-1 by targeting COX-2 and potentiated the suppression of trans-endothelial migration compared to either micro-RNA alone. These findings provide new insights on the regulation of COX-2 by micro-RNAs and shed light on the pair (miR-26b-5p and miR-101-3p) as novel prognostic and therapeutic tool that can serve to predict TNBC patients at high risk of brain metastasis and to develop novel anti-metastatic therapeutic strategies with enhanced efficacy.

The role of COX-2 in breast cancer pathogenesis has been widely studied. Cyclooxygenase enzymes catalyze the conversion of arachidonic acid to prostaglandins. The isoform COX-1 is constitutively expressed in normal tissues, whereas COX-2, undetectable in normal physiological conditions, is inducible in response to stimuli such as mitogens, cytokines, growth factors, or hormones [43]. COX-2 is overexpressed in several malignant tumors and was shown to promote carcinogenesis and cancer cell resistance to chemo- and radiotherapy [44, 45]. COX-2 overexpression converts arachidonic acid (AA) into prostaglandin E_2 (PGE2) which promotes cancer progression through inducing migration [46], stem-like cell (SLC) formation [47], and angiogenesis [48, 49]. In case of breast cancer metastasis, a number of studies showed that COX-2 expression is correlated with the metastatic spread of cancer cells and has a strong potential as prognostic indicator of disease severity and progression [50–54]. In addition, triple-negative breast cancer patients with high levels of COX-2 were found to have the greatest risk of developing brain metastasis [11]. Mechanistic studies showed that upregulation of COX-2 in TNBC metastatic cells induces MMP-1 which degrades the inter-endothelial junctions and promotes passage of cancer cells through the BBB [11–13].

Due to its important role in cancer pathogenesis, several preclinical and clinical studies tested the use of COX-2 inhibitors alone and in combination with other agents for the treatment and prevention of breast cancer, and in the adjuvant, neo-adjuvant, and metastatic treatment settings ([43, 44, 49]. Preclinical studies demonstrated that celecoxib suppress the proliferation and growth of breast cancer, while clinical studies suggested that celecoxib administration is related to reduced incidence of breast cancer in women without disease, reduced recurrence risk and mortality in women with breast cancer, and a better prognosis. However, despite promising preclinical data, trials on COX-2 inhibitors in patients with established breast tumor were unsuccessful in improving overall survival [49, 54, 55]. Similarly, clinical trials with MMP inhibitors failed to prove a survival benefit in patients with advanced disease. Batimastat, a multi-MMPs inhibitor, showed promising preclinical anti-tumor effect, however significant toxicity was observed. The clinical trials on another MMPs inhibitor, Marimastat, failed to prove a survival benefit with severe side effects. A more selective MMPs inhibitor was also tested for the treatment of metastatic lung, breast, and prostate carcinomas. However, the trials failed to demonstrate a positive effect on survival [56]. Among the possible reasons explaining the failure of COX-2 and MMP-1 inhibitors in clinical trials is that these trials were performed in patients with advanced metastatic disease, however, COX-2 and MMP-1 inhibitors are expected to be effective in early pre-metastatic stages and may not exert beneficial therapeutic effect if used in advanced stages [49, 56]. In addition, the role of COX-2 in promoting brain metastasis was documented in the TN subtype specifically [11, 12]. However, several pieces of evidence indicate that the molecular mechanism driving brain metastasis depends on the molecular subtype of BC cells. For instance, Palmiery et al., showed that HER2 overexpression promotes extravasation of HER2 + BC cells through the blood–brain barrier [57]; however TNBC do not express HER2 and therefore differences in the molecular mechanisms are evident. Therefore, COX-2 and MMP-1 inhibitors need to be tested for their metastasis preventive effect in

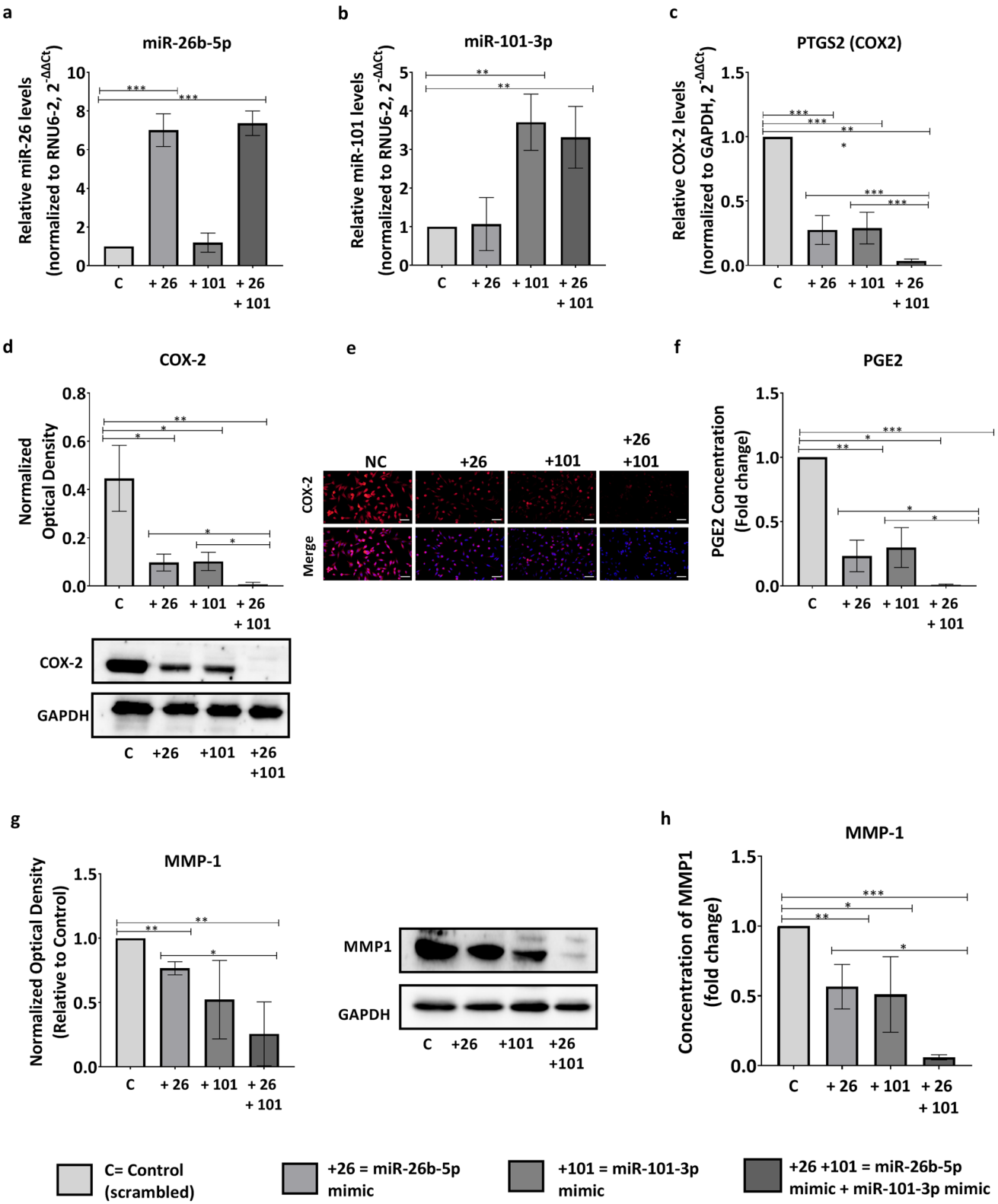
a
miR-26b-5p
Relative miR-26 levels (normalized to RNU6-2, $2^{-\Delta\Delta Ct}$)
C
+ 26
+ 101
+ 26 + 101
b
miR-101-3p
Relative miR-101 levels (normalized to RNU6-2, $2^{-\Delta\Delta Ct}$)
c
PTGS2 (COX2)
Relative COX-2 levels (normalized to GAPDH, $2^{-\Delta\Delta Ct}$)
d
COX-2
Normalized Optical Density
COX-2
GAPDH
e
NC
+26
+101
+26 +101
COX-2
Merge
f
PGE2
PGE2 Concentration (Fold change)
g
MMP-1
Normalized Optical Density (Relative to Control)
MMP1
GAPDH
h
MMP-1
Concentration of MMP1 (fold change)
C= Control (scrambled)
+26 = miR-26b-5p mimic
+101 = miR-101-3p mimic
+26 +101 = miR-26b-5p mimic + miR-101-3p mimic

◂**Fig. 6** Combination of miR-26 and miR-101 exerts a synergistic repressive effect on COX-2 expression in brain metastatic TNBC cells. MDA-MB-231-BrM2 cells were transfected with miR-26b-5p/miR-101-3p mimics or control. **a**,**b** Relative levels of miR-26b-5p (**a**) and miR-101-3p (**b**) measured by real-time PCR. The small nuclear RNA (RNU6-2) was used as an internal standard. **c** Relative levels of COX-2 (PTGS2) mRNA levels measured by real-time PCR. GAPDH was used as an internal standard. **d** Western blot analysis of COX-2 proteins. Optical densities were analyzed with Image Lab 6.0.1 software (Bio-Rad) and normalized to GAPDH. **e** Immunofluorescence staining of COX-2. **f** PGE2 levels released in the culture media quantified by ELISA. **g** Western blot analysis of MMP-1 proteins. **h** MMP-1 levels released in the culture media were quantified by ELISA. Data represent mean ± SD from three independent experiments. Scale bar = 50 µm. *$p < 0.05$, **$p < 0.01$, ***$p < 0.001$

early stages before metastases are established and in the TN subtype specifically.

However, for this strategy to become within reach, the molecular mechanisms upregulating COX-2 and MMP-1 in triple-negative breast cancer cells and rendering them more prone to disseminate to the brain need to be characterized in order to identify patients at high risk of developing brain metastasis and for better therapeutic interventions.

In this study, we identified a synergistic effect of two micro-RNAs (miR-26b-5p and miR-101-3p) in upregulating COX-2 expression in metastatic TNBC cells. miR-26b-5p and miR-101-3p are downregulated in brain metastatic cells compared to parental cells. These results are in accordance with previous studies showing that miR-26b-5p and miR-101-3p are downregulated in brain metastatic tumors compared to primary tumors in patients [29]. The roles of miR-101 and miR-26 were studied in several types of cancer [24, 58–61]. In triple-negative breast cancer cells, miR-101 was shown to exert tumor suppressor effects [62] and to increase sensitivity to paclitaxel [63]. miR-101-3p was also reported to have anti-metastatic effect in breast cancer [62–64], glioblastoma [65], lung cancer [66], hepatocellular carcinoma [67], and gallbladder carcinoma [68]. Similarly, miR-26b was shown to exert anti-tumor and anti-metastatic effects in several types of cancer including breast [26], lung [27], and human tongue carcinoma [24]. miR-26 was also found to be downregulated in advanced inflammatory breast cancer [69]. Interestingly, several studies showed that COX-2 is a direct target of miR-26b-5p and miR-101-3p. Specifically, miR-101-3p was shown to target COX-2 mRNA in endometrial carcinoma [23], colon cancer [25], and breast cancer [28], while miR-26b-5p was found to target COX-2 in breast cancer [26], lung cancer [27], and human tongue carcinoma [24]. However, role of these two micro-RNAs in regulating COX-2 expression in metastatic breast cancer cells and their dual role in brain metastasis remain to be elucidated. In a previous study, our group demonstrated that loss of miR-101-3p in metastatic breast cancer cells induces COX-2 and promotes transmigration of TNBC cells through the brain endothelium [28]. Mechanistic studies on the action of micro-RNAs reported that micro-RNAs tend to collaboratively or synergistically control gene expression [19, 21]. It was suggested that such synergistic gene regulation may maximize miRNAs' efficiency and

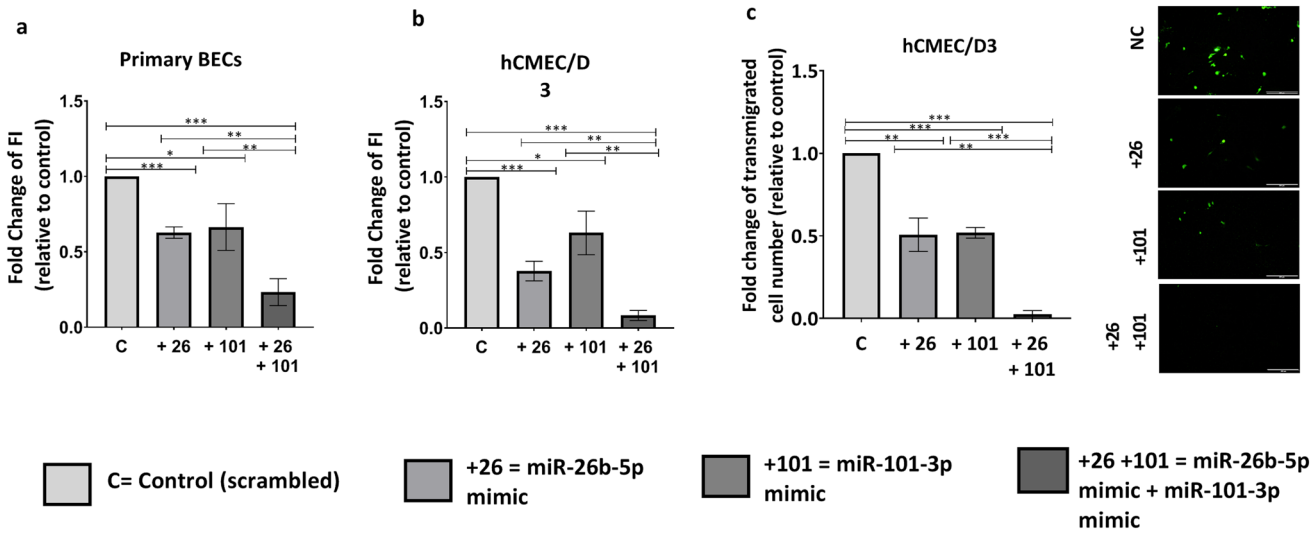

Fig. 7 Combination of miR-26 and miR-101 inhibits the transmigration of TNBC cells through the brain endothelium and preserves the endothelial barrier integrity. **a**,**b** Fluorescently labeled MDA-MB-231-BrM2 cells transfected with miR-26b-5p/miR-101-3p mimics (or control) were seeded on top of transwell inserts coated with (**a**) primary BECs or (**b**) hCMEC/D3 cells. The fluorescent intensity in the lower chambers was measured after 24 h. **c** The number of invaded cells was counted in three different fields per insert. Representative images of transmigrated cells (small green cells) are shown. Data represent mean ± SD from three independent experiments. *$p < 0.05$, **$p < 0.01$, ***$p < 0.001$

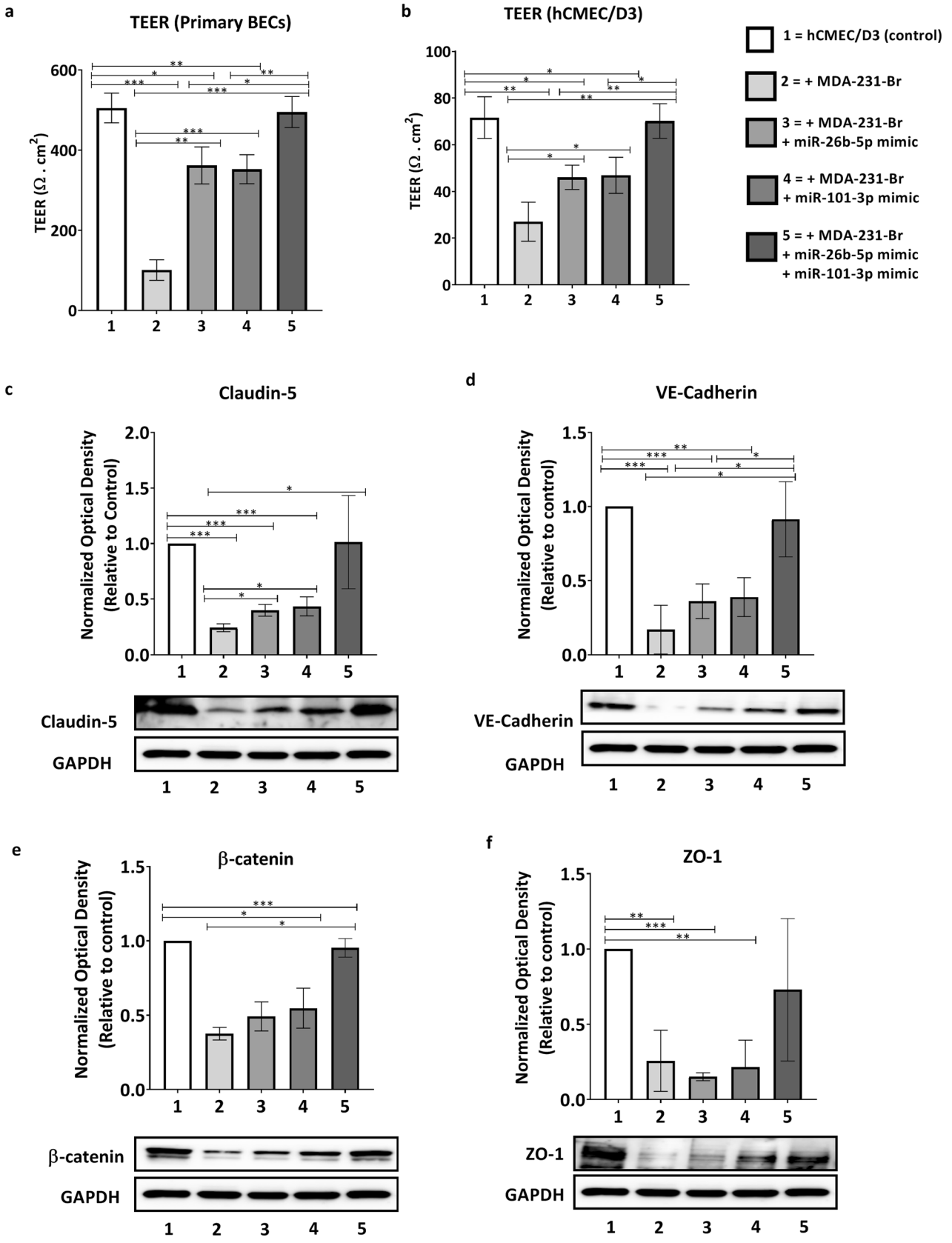
a
TEER (Primary BECs)
TEER (Ω . cm²)
b
TEER (hCMEC/D3)
TEER (Ω . cm²)
1 = hCMEC/D3 (control)
2 = + MDA-231-Br
3 = + MDA-231-Br + miR-26b-5p mimic
4 = + MDA-231-Br + miR-101-3p mimic
5 = + MDA-231-Br + miR-26b-5p mimic + miR-101-3p mimic
c
Claudin-5
Normalized Optical Density (Relative to Control)
Claudin-5
GAPDH
d
VE-Cadherin
Normalized Optical Density (Relative to control)
VE-Cadherin
GAPDH
e
β-catenin
Normalized Optical Density (Relative to control)
β-catenin
GAPDH
f
ZO-1
Normalized Optical Density (Relative to control)
ZO-1
GAPDH

◂**Fig. 8** Combination of miR-26 and miR-101 preserves the endothelial barrier integrity. **a,b** Transendothelial electrical resistance (TEER) of primary brain endothelial cells (**a**) or hCMEC/D3 (**b**) co-cultured with MDA-MB-231-BrM2 cells pre-transfected with miR-26b-5p/miR-101-3p mimics or control after 24 h of co-culture. **C–f** Western blot analysis of the inter-endothelial junctional proteins (claudin-5, VE-cadherin, β-catenin, and ZO-1) of hCMEC/D3 cells co-cultured with transfected MDA-MB-231-BrM2 cells. Optical densities were analyzed with Image Lab 6.0.1 software (Bio-Rad) and normalized to GAPDH. Data are mean ± SD from three independent experiments. $^{*}p < 0.05$, $^{**}p < 0.01$, $^{***}p < 0.001$

that the collaborative miRNA–miRNA interaction may be an important regulation mode of endogenous miRNA. As miR-26b-5p and miR-101-3p are downregulated in brain metastases and are both validated to target the 3′UTR of COX-2, we examined their potential collaboration in regulating COX-2 expression in metastatic BC cells and on tumor cells transmigrative capacity. We also tested whether a combinatorial restoration of miR-26b-5p and miR-101-3p could exert a synergistic repressive effect on COX-2 expression and suppress transmigration of TNBC cells through the brain endothelium, key step in brain metastasis. Our findings showed that the dual inhibition of both micro-RNAs (miR-26b-5p and miR-101-3p) results in higher increase of COX-2/MMP-1 and a higher transmigration of tumor cells through the brain endothelium suggesting a potential collaboration between the two micro-RNAs in the regulation of COX-2 expression. An examination of the inter-endothelial junctions revealed that the dual loss of both micro-RNAs exacerbated the disruption of the endothelial barrier compared to single inhibition. In contrast, restoration of both miR-26b-5p and miR-101-3p collaboratively targets COX-2 and exerts a synergistic repressive effect on COX-2/MMP-1. In addition, restoration of miR-26b-5p and miR-101-3p suppressed the transmigration of brain metastatic TNBC cells through the brain endothelium and preserved the barrier integrity. Importantly, the trans-endothelial suppression was potentiated when both micro-RNAs were restored simultaneously compared to single micro-RNA. These findings confirm previous reports suggesting that the simultaneous modulation of miRNA pairs exerts synergistic effects on the target genes which leads to the potentiation of their biological effects compared to single micro-RNAs.

Conclusion

The present study adds to our knowledge of the molecular mechanisms upregulating COX-2 expression in metastatic TNBC cells and granting them a higher brain propensity. Our findings imply that the pair (miR-26b-5p and miR-101-3p) could be used as a potential prognostic tool to identify TNBC patients at high risk of developing brain metastasis. In addition, we shed light on (miR-26b-5p and miR-101-3p) as potential therapeutic targets that can be exploited by subsequent in vivo and translational studies to develop better therapeutic strategies that prevent breast cancer brain metastasis to date incurable.

Supplementary Information The online version contains supplementary material available at https://doi.org/10.1007/s10549-021-06255-y.

Author contributions RH designed the study, performed research, analyzed, and interpreted the data and wrote the manuscript; AT, MM, and GK contributed to the luciferase reporter assay; AT, AM, GK, and RH provided support with analysis of data and interpretation of results. All authors read and approved the final manuscript.

Funding This work was supported by the Terry Fox Foundation's International Run Program (Grant ref. I1032). R Hamoudi is funded by Al-Jalila Foundation (Grant No: AJF201741). The funders had no role in study design, data collection and analysis, decision to publish, or preparation of the manuscript.

Data availability The authors confirm that the data supporting the findings of this study are available within the article and/or its supplementary material.

Declarations

Conflict of interest The authors declare that there are no conflicts of interest/competing interests.

Ethical approval All experiments were approved by the University of Sharjah animal care and use committee and conducted according to the UOS directives for animal care.

References

1. Kodack DP, Askoxylakis V, Ferraro GB, Fukumura D, Jain RK (2015) Emerging strategies for treating brain metastases from breast cancer. Cancer Cell 27:163–175. https://doi.org/10.1016/j.ccell.2015.01.001
2. Kennecke H, Yerushalmi R, Woods R, Cheang MCU, Voduc D, Speers CH et al (2010) Metastatic behavior of breast cancer subtypes. J Clin Oncol 28:3271–3277. https://doi.org/10.1200/JCO.2009.25.9820
3. Aversa C, Rossi V, Geuna E, Martinello R, Milani A, Redana S et al (2014) Metastatic breast cancer subtypes and central nervous system metastases. Breast 23:623–628. https://doi.org/10.1016/j.breast.2014.06.009
4. Uhm JE, Park YH, Yi SY, Cho EY, Choi YL, Lee SJ et al (2009) Treatment outcomes and clinicopathologic characteristics of triple-negative breast cancer patients who received platinum-containing chemotherapy. Int J Cancer 124:1457–1462. https://doi.org/10.1002/ijc.24090
5. Custódio-Santos T, Videira M, Brito MA (2017) Brain metastasization of breast cancer. Biochim Biophys Acta 1868:132–147. https://doi.org/10.1016/j.bbcan.2017.03.004
6. Abbott NJ, Patabendige AAK, Dolman DEM, Yusof SR, Begley DJ (2010) Structure and function of the blood–brain barrier. Neurobiol Dis 37:13–25. https://doi.org/10.1016/j.nbd.2009.07.030

7. Bauer HS, Krizbai IA, Bauer H, Traweger A (2014) "You Shall Not Pass"—tight junctions of the blood brain barrier. Front Neurosci 8:392. https://doi.org/10.3389/fnins.2014.00392
8. Rodriguez PL, Jiang S, Fu Y, Avraham S, Avraham HK (2014) The proinflammatory peptide substance P promotes blood–brain barrier breaching by breast cancer cells through changes in microvascular endothelial cell tight junctions. Int J Cancer 134:1034–1044. https://doi.org/10.1002/ijc.28433
9. Avraham HK, Jiang S, Fu Y, Nakshatri H, Ovadia H, Avraham S (2014) Angiopoietin-2 mediates blood–brain barrier impairment and colonization of triple-negative breast cancer cells in brain. J Pathol 232:369–381. https://doi.org/10.1002/path.4304
10. Lee TH, Avraham HK, Jiang S, Avraham S (2003) Vascular endothelial growth factor modulates the transendothelial migration of MDA-MB-231 breast cancer cells through regulation of brain microvascular endothelial cell permeability. J Biol Chem 278:5277–5284. https://doi.org/10.1074/jbc.M210063200
11. Wu K, Fukuda K, Xing F, Zhang Y, Sharma S, Liu Y et al (2015) Roles of the cyclooxygenase 2 matrix metalloproteinase 1 pathway in brain metastasis of breast cancer. J Biol Chem 290:9842–9854. https://doi.org/10.1074/jbc.M114.602185
12. Bos PD, Zhang XHF, Nadal C, Shu W, Gomis RR, Nguyen DX et al (2009) Genes that mediate breast cancer metastasis to the brain. Nature 459:1005–1009. https://doi.org/10.1038/nature08021
13. Liu H, Kato Y, Erzinger SA, Kiriakova GM, Qian Y, Palmieri D et al (2012) The role of MMP-1 in breast cancer growth and metastasis to the brain in a xenograft model. BMC Cancer 12:583. https://doi.org/10.1186/1471-2407-12-583
14. He L, Hannon GJ (2004) MicroRNAs: small RNAs with a big role in gene regulation. Nat Rev Genet 5:522–531. https://doi.org/10.1038/nrg1379
15. Rupaimoole R, Slack FJ (2017) MicroRNA therapeutics: towards a new era for the management of cancer and other diseases. Nat Rev Drug Discov 16:203–222. https://doi.org/10.1038/nrd.2016.246
16. Oliveto S, Mancino M, Manfrini N, Biffo S (2017) Role of microRNAs in translation regulation and cancer. World J Biol Chem 8:45. https://doi.org/10.4331/wjbc.v8.i1.45
17. Kulyte A, Belarbi Y, Lorente-Cebrian S, Bambace C, Arner E, Daub CO et al (2014) Additive effects of microRNAs and transcription factors on CCL2 production in human white adipose tissue. Diabetes 63:1248–1258. https://doi.org/10.2337/db13-0702
18. Xu Y, Zhu W, Wang Z, Yuan W, Sun Y, Liu H et al (2015) Combinatorial microRNAs suppress hypoxia-induced cardiomyocytes apoptosis. Cell Physiol Biochem 37:921–932. https://doi.org/10.1159/000430219
19. Zhang J, Pham VVH, Liu L, Xu T, Truong B, Li J et al (2019) Identifying miRNA synergism using multiple-intervention causal inference. BMC Bioinform 20:613. https://doi.org/10.1186/s12859-019-3215-5
20. Vandenwijngaert S, Ledsky CD, Agha O, Wu C, Hu D, Bagchi A et al (2018) MicroRNA-425 and microRNA-155 cooperatively regulate atrial natriuretic peptide expression and cGMP production. PLoS ONE 13:e0196697. https://doi.org/10.1371/journal.pone.0196697
21. Chen X, Zhao W, Yuan Y, Bai Y, Sun Y, Zhu W et al (2017) MicroRNAs tend to synergistically control expression of genes encoding extensively-expressed proteins in humans. PeerJ 5:e3682. https://doi.org/10.7717/peerj.3682
22. Zhu W, Zhao Y, Xu Y, Sun Y, Wang Z, Yuan W et al (2013) Dissection of protein interactomics highlights microRNA synergy. PLoS ONE 8:e63342. https://doi.org/10.1371/journal.pone.0063342
23. Liu Y, Li H, Zhao C, Jia H (2018) MicroRNA-101 inhibits angiogenesis via COX-2 in endometrial carcinoma. Mol Cell Biochem 448:61–69. https://doi.org/10.1007/s11010-018-3313-0
24. Cao J, Guo T, Dong Q, Zhang J, Li Y (2015) miR-26b is downregulated in human tongue squamous cell carcinoma and regulates cell proliferation and metastasis through a COX-2-dependent mechanism. Oncol Rep 33:974–980. https://doi.org/10.3892/or.2014.3648
25. Strillacci A, Griffoni C, Sansone P, Paterini P, Piazzi G, Lazzarini G et al (2009) MiR-101 downregulation is involved in cyclooxygenase-2 overexpression in human colon cancer cells. Exp Cell Res 315:1439–1447. https://doi.org/10.1016/j.yexcr.2008.12.010
26. Li J, Kong X, Zhang J, Luo Q, Li X, Fang L (2013) MiRNA-26b inhibits proliferation by targeting PTGS2 in breast cancer. Cancer Cell Int 13:7. https://doi.org/10.1186/1475-2867-13-7
27. Xia M, Duan ML, Tong JH, Xu JG (2015) MiR-26b suppresses tumor cell proliferation, migration and invasion by directly targeting COX-2 in lung cancer. Eur Rev Med Pharmacol Sci 19(24):4728–4737
28. Harati R, Mohammad MG, Tlili A, El-Awady RA, Hamoudi R (2020) Loss of miR-101-3p promotes transmigration of metastatic breast cancer cells through the brain endothelium by inducing COX-2/MMP1 signaling. Pharmaceuticals 13:144. https://doi.org/10.3390/ph13070144
29. Xing F, Sharma S, Liu Y, Mo YY, Wu K, Zhang YY et al (2015) miR-509 suppresses brain metastasis of breast cancer cells by modulating RhoC and TNF-α. Oncogene 34:4890–4900. https://doi.org/10.1038/onc.2014.412
30. Weksler B, Romero IA, Couraud PO (2013) The hCMEC/D3 cell line as a model of the human blood brain barrier. Fluids Barriers CNS 10:16. https://doi.org/10.1186/2045-8118-10-16
31. Poller B, Gutmann H, Krähenbühl S, Weksler B, Romero I, Couraud P-O et al (2008) The human brain endothelial cell line hCMEC/D3 as a human blood-brain barrier model for drug transport studies. J Neurochem 107:1358–1368. https://doi.org/10.1111/j.1471-4159.2008.05730.x
32. Harati R, Benech H, Villégier AS, Mabondzo A (2013) P-Glycoprotein, breast cancer resistance protein, organic anion transporter 3, and transporting peptide 1a4 during blood-brain barrier maturation: involvement of wnt/β-catenin and endothelin-1 signaling. Mol Pharm 10:1566–1580. https://doi.org/10.1021/mp300334r
33. Harati R, Villégier A-S, Banks WA, Mabondzo A (2012) Susceptibility of juvenile and adult blood–brain barrier to endothelin-1: regulation of P-glycoprotein and breast cancer resistance protein expression and transport activity. J Neuroinflammation 9:765. https://doi.org/10.1186/1742-2094-9-273
34. Livak KJ, Schmittgen TD (2001) Analysis of relative gene expression data using real-time quantitative PCR and the $2-\Delta\Delta CT$ method. Methods 25:402–408. https://doi.org/10.1006/meth.2001.1262
35. Harati R, Hafezi S, Mabondzo A, Tlili A (2020) Silencing miR-202-3p increases MMP-1 and promotes a brain invasive phenotype in metastatic breast cancer cells. PLoS ONE 15:e0239292–e0239292. https://doi.org/10.1371/journal.pone.0239292
36. Rodrigues-Ferreira S, Abdelkarim M, Dillenburg-Pilla P, Luissint AC, di Tommaso A, Deshayes F et al (2012) Angiotensin II facilitates breast cancer cell migration and metastasis. PLoS ONE 7:e35667. https://doi.org/10.1371/journal.pone.0035667
37. Fu J, Zhang N, Chou JH, Dong HJ, Lin SF, Ulrich-Merzenich GS et al (2016) Drug combination in vivo using combination index method: taxotere and T607 against colon carcinoma HCT-116 xenograft tumor in nude mice. Synergy 3:15–30. https://doi.org/10.1016/j.synres.2016.06.001
38. Chou TC (2006) Theoretical basis, experimental design, and computerized simulation of synergism and antagonism in drug

combination studies. Pharmacol Rev 58:621. https://doi.org/10.1124/pr.58.3.10
39. Chou TC (2018) The combination index (CI < 1) as the definition of synergism and of synergy claims. Synergy 7:49–50. https://doi.org/10.1016/j.synres.2018.04.001
40. Yadav SS, Li J, Stockert JA, O'Connor J, Herzog B, Elaiho C et al (2016) Combination effect of therapies targeting the PI3K- and AR-signaling pathways in prostate cancer. Oncotarget 7:76181–76196. https://doi.org/10.18632/oncotarget.12771
41. Lai X, Eberhardt M, Schmitz U, Vera J (2019) Systems biology-based investigation of cooperating microRNAs as monotherapy or adjuvant therapy in cancer. Nucleic Acids Res 47:7753–7766. https://doi.org/10.1093/nar/gkz638
42. Jin HY, Gonzalez-Martin A, Miletic AV, Lai M, Knight S, Sabouri-Ghomi M et al (2015) Transfection of microRNA mimics should be used with caution. Front Genet. https://doi.org/10.3389/fgene.2015.00340
43. Mazhar D, Ang R, Waxman J (2006) COX inhibitors and breast cancer. Br J Cancer 94:346–350. https://doi.org/10.1038/sj.bjc.6602942
44. Hashemi Goradel N, Najafi M, Salehi E, Farhood B, Mortezaee K (2019) Cyclooxygenase-2 in cancer: a review. J Cell Physiol 234:5683–5699. https://doi.org/10.1002/jcp.27411
45. Boland GP, Butt IS, Prasad R, Knox WF, Bundred NJ (2004) COX-2 expression is associated with an aggressive phenotype in ductal carcinoma in situ. Br J Cancer 90:423–429. https://doi.org/10.1038/sj.bjc.6601534
46. Timoshenko AV, Xu G, Chakrabarti S, Lala PK, Chakraborty C (2003) Role of prostaglandin E2 receptors in migration of murine and human breast cancer cells. Exp Cell Res 289:265–274. https://doi.org/10.1016/S0014-4827(03)00269-6
47. Majumder M, Xin X, Liu L, Girish GV, Lala PK (2014) Prostaglandin E2 receptor EP4 as the common target on cancer cells and macrophages to abolish angiogenesis, lymphangiogenesis, metastasis, and stem-like cell functions. Cancer Sci 105:1142–1151. https://doi.org/10.1111/cas.12475
48. Chang SH, Liu CH, Conway R, Han DK, Nithipatikom K, Trifan OC et al (2004) Role of prostaglandin E2-dependent angiogenic switch in cyclooxygenase 2-induced breast cancer progression. Proc Natl Acad Sci 101(2):591–596. https://doi.org/10.1073/pnas.2535911100
49. Li J, Hao Q, Cao W, Vadgama JV, Wu Y (2018) Celecoxib in breast cancer prevention and therapy. Cancer Manag Res 10:4653–4667. https://doi.org/10.2147/CMAR.S178567
50. Denkert C, Winzer KJ, Müller BM, Weichert W, Pest S, Köbel M et al (2003) Elevated expression of cyclooxygenase-2 is a negative prognostic factor for disease free survival and overall survival in patients with breast carcinoma. Cancer 97:2978–2987. https://doi.org/10.1002/cncr.11437
51. Shim JY, An HJ, Lee YH, Kim SK, Lee KP, Lee KS (2003) Overexpression of cyclooxygenase-2 Is associated with breast carcinoma and its poor prognostic factors. Mod Pathol 16:1199–1204. https://doi.org/10.1097/01.MP.0000097372.73582.CB
52. Tan KB, Yong WP, Putti TC (2004) Cyclooxygenase-2 expression: a potential prognostic and predictive marker for high-grade ductal carcinoma in situ of the breast. Histopathology 44:24–28. https://doi.org/10.1111/j.1365-2559.2004.01774.x
53. Perrone G, Santini D, Vincenzi B, Zagami M, La Cesa A, Bianchi A et al (2005) COX-2 expression in DCIS: correlation with VEGF, HER-2/neu, prognostic molecular markers and clinicopathological features. Histopathology 46:561–568. https://doi.org/10.1111/j.1365-2559.2005.02132.x
54. Harris RE (2014) Cyclooxygenase-2 and the inflammogenesis of breast cancer. World J Clin Oncol 5:677. https://doi.org/10.5306/wjco.v5.i4.677
55. Zhang Z, Chen F, Shang L (2018) Advances in antitumor effects of NSAIDs. Cancer Manag Res 10:4631–4640. https://doi.org/10.2147/CMAR.S175212
56. Winer A, Adams S, Mignatti P (2018) Matrix metalloproteinase inhibitors in cancer therapy: turning past failures into future successes. Mol Cancer Ther 17:1147–1155. https://doi.org/10.1158/1535-7163.MCT-17-0646
57. Palmieri D, Bronder JL, Herring JM, Yoneda T, Weil RJ, Stark AM et al (2007) Her-2 overexpression increases the metastatic outgrowth of breast cancer cells in the brain. Cancer Res 67:4190–4198. https://doi.org/10.1158/0008-5472.CAN-06-3316
58. He Y, Liu H, Jiang L, Rui B, Mei J, Xiao H (2019) miR-26 induces apoptosis and inhibits autophagy in non-small cell lung cancer cells by suppressing TGF-β1-JNK signaling pathway. Front Pharmacol 9:1509. https://doi.org/10.3389/fphar.2018.01509
59. Wang XJ, Yan ZJ, Luo GC, Chen YY, Bai PM (2020) miR-26 suppresses renal cell cancer via down-regulating coronin-3. Mol Cell Biochem 463:137–146. https://doi.org/10.1007/s11010-019-03636-2
60. Li J, Liang Y, Lv H, Meng H, Xiong G, Guan X et al (2017) miR-26a and miR-26b inhibit esophageal squamous cancer cell proliferation through suppression of c-MYC pathway. Gene 625:1–9. https://doi.org/10.1016/j.gene.2017.05.001
61. Zhu L, Chen Y, Nie K, Xiao Y, Yu H (2018) MiR-101 inhibits cell proliferation and invasion of pancreatic cancer through targeting STMN1. Cancer Biomark 23:301–309. https://doi.org/10.3233/CBM-181675
62. Liu P, Ye F, Xie X, Li X, Tang H, Li S et al (2016) mir-101–3p is a key regulator of tumor metabolism in triple negative breast cancer targeting AMPK. Oncotarget 7(23):35188–35198. https://doi.org/10.18632/oncotarget.9072
63. Liu X, Tang H, Chen J, Song C, Yang L, Liu P et al (2015) MicroRNA-101 inhibits cell progression and increases paclitaxel sensitivity by suppressing MCL-1 expression in human triple-negative breast cancer. Oncotarget 6:20070–20083. https://doi.org/10.18632/oncotarget.4039
64. Zhang X, Gao D, Fang K, Guo Z, Li L (2019) Med19 is targeted by miR-101–3p/miR-422a and promotes breast cancer progression by regulating the EGFR/MEK/ERK signaling pathway. Cancer Lett 444:105–115. https://doi.org/10.1016/j.canlet.2018.12.008
65. Li L, Shao MY, Zou SC, Xiao ZF, Chen ZC (2019) MiR-101-3p inhibits EMT to attenuate proliferation and metastasis in glioblastoma by targeting TRIM44. J Neurooncol 141:19–30. https://doi.org/10.1007/s11060-018-2973-7
66. Han L, Chen W, Xia Y, Song Y, Zhao Z, Cheng H et al (2018) MiR-101 inhibits the proliferation and metastasis of lung cancer by targeting zinc finger E-box binding homeobox1. Am J Transl Res 10(4):1172–1183
67. Yan S, Shan X, Chen K, Liu Y, Yu G, Chen Q et al (2018) LINC00052/miR-101-3p axis inhibits cell proliferation and metastasis by targeting SOX9 in hepatocellular carcinoma. Gene 679:138–149. https://doi.org/10.1016/j.gene.2018.08.038
68. Bao RF, Shu YJ, Hu YP, Wang XA, Zhang F, Liang HB et al (2016) miR-101 targeting ZFX suppresses tumor proliferation and metastasis by regulating the MAPK/Erk and Smad pathways in gallbladder carcinoma. Oncotarget 7:22339–22354. https://doi.org/10.18632/oncotarget.7970
69. Ding Q, Wang Y, Zuo Z, Gong Y, Krishnamurthy S, Li CW et al (2018) Decreased expression of microRNA-26b in locally advanced and inflammatory breast cancer. Hum Pathol 77:121–129. https://doi.org/10.1016/j.humpath.2018.04.002